NASA/TM-2009-214646

Updating the Finite Element Model of the Aerostructures Test Wing Using Ground Vibration Test Data

Shun-Fat Lung
TYBRIN Inc.
Edwards, California

Chan-Gi Pak
NASA Dryden Flight Research Center
Edwards, California

April 2009

NASA STI Program ... in Profile

Since its founding, NASA has been dedicated to the advancement of aeronautics and space science. The NASA scientific and technical information (STI) program plays a key part in helping NASA maintain this important role.

The NASA STI program operates under the auspices of the Agency Chief Information Officer. It collects, organizes, provides for archiving, and disseminates NASA's STI. The NASA STI program provides access to the NASA Aeronautics and Space Database and its public interface, the NASA Technical Report Server, thus providing one of the largest collections of aeronautical and space science STI in the world. Results are published in both non-NASA channels and by NASA in the NASA STI Report Series, which includes the following report types:

- TECHNICAL PUBLICATION. Reports of completed research or a major significant phase of research that present the results of NASA Programs and include extensive data or theoretical analysis. Includes compilations of significant scientific and technical data and information deemed to be of continuing reference value. NASA counterpart of peer-reviewed formal professional papers but has less stringent limitations on manuscript length and extent of graphic presentations.

- TECHNICAL MEMORANDUM. Scientific and technical findings that are preliminary or of specialized interest, e.g., quick release reports, working papers, and bibliographies that contain minimal annotation. Does not contain extensive analysis.

- CONTRACTOR REPORT. Scientific and technical findings by NASA-sponsored contractors and grantees.

- CONFERENCE PUBLICATION. Collected papers from scientific and technical conferences, symposia, seminars, or other meetings sponsored or co-sponsored by NASA.

- SPECIAL PUBLICATION. Scientific, technical, or historical information from NASA programs, projects, and missions, often concerned with subjects having substantial public interest.

- TECHNICAL TRANSLATION. English-language translations of foreign scientific and technical material pertinent to NASA's mission.

Specialized services also include creating custom thesauri, building customized databases, and organizing and publishing research results.

For more information about the NASA STI program, see the following:

- Access the NASA STI program home page at *http://www.sti.nasa.gov*

- E-mail your question via the Internet to help@sti.nasa.gov

- Fax your question to the NASA STI Help Desk at 443-757-5803

- Phone the NASA STI Help Desk at 443-757-5802

- Write to:
  NASA STI Help Desk
  NASA Center for AeroSpace Information
  7115 Standard Drive
  Hanover, MD 21076-1320

NASA/TM-2009-214646

Updating the Finite Element Model of the Aerostructures Test Wing Using Ground Vibration Test Data

Shun-Fat Lung
TYBRIN Inc.
Edwards, California

Chan-Gi Pak
NASA Dryden Flight Research Center
Edwards, California

National Aeronautics and
Space Administration

Dryden Flight Research Center
Edwards, California 93523-0273

April 2009

ACKNOWLEDGEMENT

The authors would like to acknowledge the assistance of Claudia Herrara, Matt Moholt and Starr Ginn at NASA Dryden Flight Research Center in the setting and performing of the ground vibration tests.

Available from:

NASA Center for AeroSpace Information
7115 Standard Drive
Hanover, MD 21076-1320
(301) 621-0390

ABSTRACT

Improved and/or accelerated decision making is a crucial step during flutter certification processes. Unfortunately, most finite element structural dynamics models have uncertainties associated with model validity. Tuning the finite element model using measured data to minimize the model uncertainties is a challenging task in the area of structural dynamics. The model tuning process requires not only satisfactory correlations between analytical and experimental results, but also the retention of the mass and stiffness properties of the structures. Minimizing the difference between analytical and experimental results is a type of optimization problem. By utilizing the multidisciplinary design, analysis, and optimization (MDAO) tool in order to optimize the objective function and constraints; the mass properties, the natural frequencies, and the mode shapes can be matched to the target data to retain the mass matrix orthogonality. This approach has been applied to minimize the model uncertainties for the structural dynamics model of the aerostructures test wing (ATW), which was designed and tested at the National Aeronautics and Space Administration Dryden Flight Research Center (Edwards, California). This study has shown that natural frequencies and corresponding mode shapes from the updated finite element model have excellent agreement with corresponding measured data.

NOMENCLATURE

AR	aspect ratio
ATW	aerostructures test wing
CG	center of gravity
DFRC	Dryden Flight Research Center
DOF	degrees of freedom
DPR	driving point residues
d	number of degrees of freedom
$\boldsymbol{E}$	effective independent matrix
EI	effective independence
F	original objective function
FE	finite element
FIM	Fisher information matrix
G	subscript for target values (or measured quantities)
GA	genetic algorithm
GVT	ground vibration test
g_i	inequality constraints
h_j	equality constraints
I_{XX}	computed x moment of inertia about the center of gravity
I_{XXG}	target x moment of inertia about the center of gravity
I_{xy}	computed xy moment of inertia about the center of gravity
I_{XYG}	target xy moment of inertia about the center of gravity
I_{YY}	computed y moment of inertia about the center of gravity
I_{YYG}	target y moment of inertia about the center of gravity
I_{YZ}	computed yz moment of inertia about the center of gravity
I_{YZG}	target yz moment of inertia about the center of gravity
I_{ZX}	computed zx moment of inertia about the center of gravity

I_{ZXG}	target zx moment of inertia about the center of gravity
I_{ZZ}	computed z moment of inertia about the center of gravity
I_{ZZG}	target z moment of inertia about the center of gravity
J_i	objective functions (optimization problem statement number i = 1, 2, … , 13)
$\mathbf{K}$	stiffness matrix
$\overline{\mathbf{K}}$	orthonormalized stiffness matrix
KE	kinetic energy
KE_{ik}	kinetic energy associated with the *i*-th DOF in the *k*-th target mode
L	new objective function
l	number of modes
$\mathbf{M}$	mass matrix
$\overline{\mathbf{M}}$	orthonormalized mass matrix
MAC	modal assurance criterion
MDAO	multidisciplinary design, analysis and optimization
m	number of sensors (or number of measured degrees of freedom)
n	number of modes to be matched
q	number of inequality constraints
r	number of equality constraints
SEREP	system equivalent reduction expansion process
SMI	structural mode interaction
$\mathbf{T}$	transformation matrix
W	computed total mass
W_G	target total mass
X	x-coordinate of computed center of gravity
$\overline{X}$	design variables vector
X_G	x-coordinate of target center of gravity
Y	y-coordinate of computed center of gravity
Y_G	y-coordinate of target center of gravity
Z	z-coordinate of computed center of gravity
Z_G	z-coordinate of target center of gravity
ε	small tolerance value for inequality constraints
λ	Lagrange multiplier
$\mathbf{\Phi}$	computed eigen-matrix ($m \times n$)
$\mathbf{\Phi_G}$	target eigen-matrix ($m \times n$)
$\overline{\mathbf{\Phi}}$	Reduced modal matrix ($d \times l$)
ϕ_i	i-th mode shape ($d \times 1$)
Ω_j	j-th computed frequency
ω_k	corresponding natural frequency

INTRODUCTION

A test article called the aerostructures test wing (ATW) was developed and flown at the National Aeronautics and Space Administration (NASA) Dryden Flight Research Center (DFRC) (Edwards, California) on the McDonnell Douglas NF15B test bed aircraft as shown in figure 1 for the purpose of demonstrating and validating flutter prediction methods during flight (ref. 1). The first aerostructures test wing (ATW1), flown in 2001, was originally developed to directly address requests for better flight flutter test techniques by providing a functional flight test platform. While the first series of tests was extremely successful, the minimum amount of instrumentation (structural accelerometers and strain gages) was chosen to satisfy the scope of the program. These sensors were limited in their capability to answer questions of aeroelastic interactions, sources of nonlinearity, physical mechanisms of aeroelastic coupling, and feedback dynamics between the structure and aerodynamics.

090060

Figure 1. Aerostructures test wing mounted on the NF15B for flight flutter testing.

A second aerostructures test wing (ATW2), as shown in figure 2, was built for the demonstration of state-of-the-art sensor technologies for simultaneous; distributed; collocated measurement of shear stress (skin friction); steady and unsteady pressures; and structural strain and accelerations for mode shapes as well as other modal properties. Like the ATW1, the ATW2 was flown on the NF15B aircraft. In order to have a successful prediction of the onset flutter, the structural dynamics finite element (FE) model has to be robust and accurate. The ground vibration test (GVT) is used as one of the validation methods for robustness of the FE model.

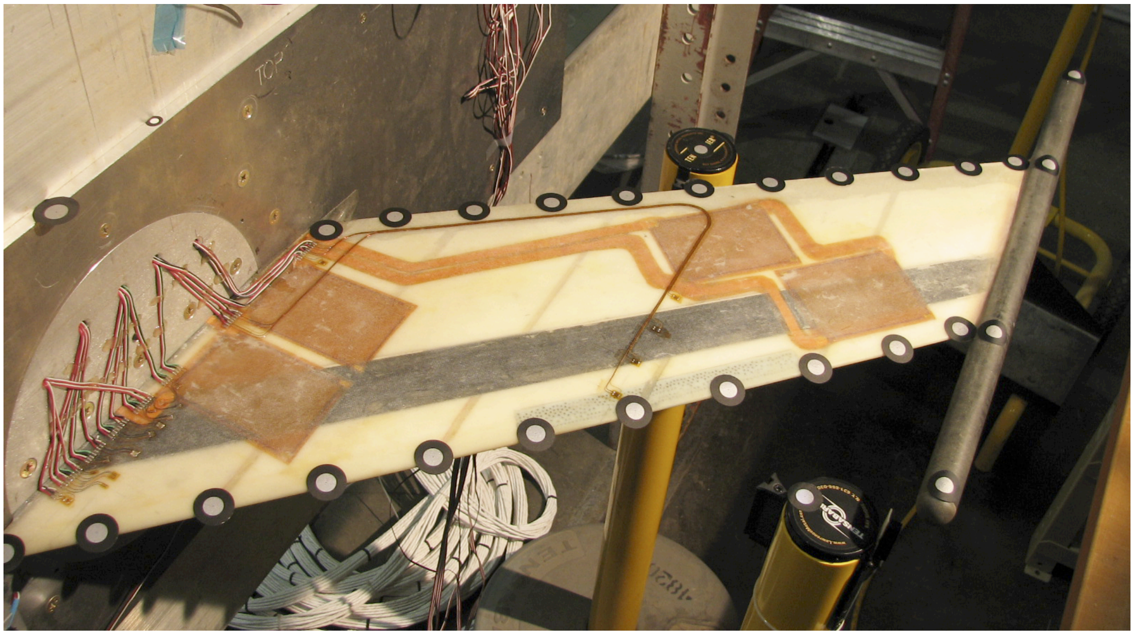

090061

Figure 2. Aerostructures test wing 2.

The primary objective of this study is to obtain the GVT validated structural dynamics FE model for minimizing model uncertainties in the predicted flutter boundaries. Discrepancies are common between the test data and the analytical results. However, the FE model can be fine tuned through the use of the GVT data. Accurate and reliable GVT results are important to this adjusting process. Selection of measurement locations can be critical to the success of an experimental modal survey. So, different sensor and exciter placement algorithms for pre-test evaluations were investigated to ensure the quality of the modal test.

Manual trial-and-error methods provide an inefficient approach to correlate the FE model with test data. A more efficient approach is to use a mode matching technique for the model refinement of both ground and flight-based models. A model tuning technique utilized was NASA Dryden's multidisciplinary design, analysis, and optimization (MDAO) tool (ref. 2), which was used to adjust the structural properties so that the analytical results and the measured data were matched.

SENSOR/ACTUATOR PLACEMENT METHODS

It is important to assure that an adequate number of proper sensor locations are identified for the collection of data during the GVT. There are several existing techniques that can be used for the determination of measurement locations. These algorithms start with a full or selected set of finite element degrees of freedom (DOFs) with the desired number of mode shapes as shown in equation (1):

$$\overline{\Phi} = [\phi_1 \phi_2 \ldots \phi_l] \tag{1}$$

where $\overline{\Phi}$ is the reduced modal matrix ($d \times l$). Depending on the algorithm, the unwanted DOFs can be eliminated in one cycle or iteratively until the desired number of sensors is reached.

Effective Independence

The objective of the effective independence (EI) method is to select sensor locations that make the target modes linearly independent, while retaining as much information as possible. This procedure starts from a large set of candidate sensor locations in which the effective independence matrix ***E*** can be formed as shown in equation (2) (ref. 3).

$$\boldsymbol{E} = \overline{\Phi}\left(\overline{\Phi}^T\overline{\Phi}\right)^{-1}\overline{\Phi}^T \tag{2}$$

The DOF with the smallest value is removed and the ***E*** matrix is re-calculated for the new candidate set. The iterative process continues until the desired number of sensors is reached.

Genetic Algorithm

Selection of the sensor locations is a kind of optimization problem with discrete design variables. One of the solution methods for this optimization problem is the genetic algorithm (GA) (ref. 4). Using the determinant of the Fisher information matrix (**FIM**) as objective function, and sensor locations as design variables, the optimal sensor locations can be determined. The **FIM** is defined as shown in equation (3) (ref. 5).

$$\mathbf{FIM} \equiv \overline{\Phi}^T\overline{\Phi} \tag{3}$$

The sensor locations, which are based on the desired number of sensors, are randomly picked and the GA method will find the best set of locations that gives the maximum determinant value of the **FIM**. The determinant of the **FIM** indicates the amount of information in the data that is retained at the reduced set of coordinates. Maintaining a high value for this determinant is desired so that the **FIM** retains as much information as possible. The optimization problem statement can be written as:

Maximize the objective function $obj = \det(\mathbf{FIM})$ for any set of sensor positions with no constraint equations.

Kinetic Energy Sorting

The kinetic energy sorting technique involves an examination of each DOF's contribution of kinetic energy to each mode shape. The calculation of the kinetic energy in terms of the mode shapes can be expressed as shown in equation (4):

$$\mathrm{KE}_{ik} = \overline{\Phi}_{ik}\sum_j \mathrm{M}_{ij}\overline{\Phi}_{jk} \tag{4}$$

where KE_{ik} is the kinetic energy associated with the *i*-th DOF in the *k*-th target mode. The total kinetic energy for each DOF is the summation of the normalized kinetic energy of each DOF for each mode. Those DOFs having the greatest contribution or most kinetic energy can be identified and selected as sensor locations.

Guyan Reduction

The purpose of the Guyan reduction (ref. 6) is to remove the number of DOFs in a large FE model, but still maintain the characteristics of the original model at the lower frequencies. Higher frequency modes are neglected because these DOFs can be removed based on the fact that the inertia forces are negligible compared with the elastic forces. This process involves examining the ratio of stiffness over mass for each DOF. If the ratio is small, then there are significant inertia effects associated with the DOF, and thus it should be retained. If the ratio is large, then the inertia effects are negligible and the corresponding DOF can be removed.

Iterative Guyan Reduction

Unlike the standard Guyan reduction, the iterative Guyan reduction (ref. 7) removes the DOF one at a time so that at each stage the effect of each DOF removed is redistributed to all of the remaining DOFs, resulting in greater accuracy than the non-iterative approach.

Driving Point Residues

Driving point residues (DPR) are equivalent to modal participation factors. They are proportional to the magnitude of the mode shapes. A driving point is a point in the structure where the excitation DOF and the response are equal. If the modal matrix is mass normalized, then the driving point residues for the DOF *i* of the mode shape *k* can be computed (ref. 8) as shown in equation (5):

$$DPR_k(i,i) = \frac{\bar{\Phi}(i) \otimes \bar{\Phi}(i)}{\omega_k} \tag{5}$$

where ω_k is the corresponding natural frequency and $\otimes$ is the element-by-element multiplication operator. The normalized DPR can then be used to calculate the average, minimum, maximum, and weighted modal displacement of all the target modes. The optimal sensor/exciter locations are then selected based on the values of the weighted driving point residue and the number of sensors/actuators available for the test. In this study, the weighted minimum was used for the selection of the sensor locations in order to opt out of those DOFs at the nodal point of a mode. The weighted minimum DPR was obtained as shown in equation (6).

$$DPR_{weighted}(i) = \min_{j=1}^{n} \overline{DPR}_j(i,i) \cdot \frac{1}{n} \sum_{j=1}^{n} \overline{DPR}_j(i,i) \tag{6}$$

The weighted maximum was used for the selection of the excitation locations so that those easily excited DOFs could be identified. The weighted maximum DPR can be expressed as shown in equation (7):

$$DPR_{weighted}(i) = \max_{j=1}^{n} \overline{DPR}_j(i,i) \cdot \frac{1}{n} \sum_{j=1}^{n} \overline{DPR}_j(i,i) \tag{7}$$

where $\overline{DPR}$ is the normalized DPR.

STRUCTURAL DYNAMIC MODEL TUNING PROCEDURE

Discrepancies in frequencies and mode shapes are minimized using a series of optimization procedures (refs. 9-11). There are two optimization algorithms adopted in NASA Dryden's MDAO tool: the traditional gradient-based algorithm (ref. 12) and the genetic algorithm. Gradient-based algorithms work well for continuous design variable problems, whereas GAs can handle continuous and discrete design variable problems easily. When there are multiple local minima, GAs are able to find the global optimum results, whereas gradient-based methods may converge to a locally minimum value. In this research work, the GA was used for the solution of the optimization problem.

The GA is directly applicable only to unconstrained optimization; it is necessary to use some additional methods in order to solve the constrained optimization problem. The most popular approach is to add penalty functions in proportion to the magnitude of constraint violation to the objective function (ref. 13). The general form of the penalty function is shown in equation (8):

$$\mathrm{L}(\bar{\mathrm{X}}) = \mathrm{F}(\bar{\mathrm{X}}) + \sum_{i=1}^{q} \lambda_i \mathrm{g}_i\left(\bar{\mathrm{X}}\right) + \sum_{j=1}^{r} \lambda_{j+q} \mathrm{h}_j\left(\bar{\mathrm{X}}\right) \tag{8}$$

where $\mathrm{L}(\bar{\mathrm{X}})$ indicates the new objective function to be optimized, $\mathrm{F}(\bar{\mathrm{X}})$ is the original objective function, $\mathrm{g}_i(\bar{\mathrm{X}})$ is the inequality constraint, $\mathrm{h}_j(\bar{\mathrm{X}})$ is the equality constraint, λ_i are the Lagrange multipliers, $\bar{\mathrm{X}}$ is the design variables vector, and q and r are the number of inequality and equality constraints, respectively.

The analytical mass properties, the mass matrix orthogonality, and the natural frequencies and mode shapes are matched to the target values based on the following three tuning steps.

Step 1: Tuning Mass Properties

The difference in the analytical and target values of the total mass, the center of gravity (CG) location, and the mass moment of inertias at the CG location are minimized to have the improved rigid body dynamics as shown in equations (9) through (18).

$$\mathrm{J}_1 = (\mathrm{W} - \mathrm{W}_G)^2 / \mathrm{W}_G^2 \tag{9}$$

$$\mathrm{J}_2 = (\mathrm{X} - \mathrm{X}_G)^2 / \mathrm{X}_G^2 \tag{10}$$

$$\mathrm{J}_3 = (\mathrm{Y} - \mathrm{Y}_G)^2 / \mathrm{Y}_G^2 \tag{11}$$

$$\mathrm{J}_4 = (\mathrm{Z} - \mathrm{Z}_G)^2 / \mathrm{Z}_G^2 \tag{12}$$

$$\mathrm{J}_5 = (\mathrm{I}_{\mathrm{XX}} - \mathrm{I}_{\mathrm{XX}G})^2 / \mathrm{I}_{\mathrm{XX}G}^2 \tag{13}$$

$$\mathrm{J}_6 = (\mathrm{I}_{\mathrm{YY}} - \mathrm{I}_{\mathrm{YY}G})^2 / \mathrm{I}_{\mathrm{YY}G}^2 \tag{14}$$

$$\mathrm{J}_7 = (\mathrm{I}_{\mathrm{ZZ}} - \mathrm{I}_{\mathrm{ZZ}G})^2 / \mathrm{I}_{\mathrm{ZZ}G}^2 \tag{15}$$

$$\mathrm{J}_8 = (\mathrm{I}_{\mathrm{XY}} - \mathrm{I}_{\mathrm{XY}G})^2 / \mathrm{I}_{\mathrm{XY}G}^2 \tag{16}$$

$$\mathrm{J}_9 = (\mathrm{I}_{\mathrm{YZ}} - \mathrm{I}_{\mathrm{YZ}G})^2 / \mathrm{I}_{\mathrm{YZ}G}^2 \tag{17}$$

$$\mathrm{J}_{10} = (\mathrm{I}_{\mathrm{ZX}} - \mathrm{I}_{\mathrm{ZX}G})^2 / \mathrm{I}_{\mathrm{ZX}G}^2 \tag{18}$$

Step 2: Tuning Mass Matrix

The off-diagonal terms of the orthonormalized mass matrix are reduced to improve the mass orthogonality as shown in equation (19):

$$J_{11} = \sum_{i=1,\, j=1,\, i \neq j}^{n} \left(\overline{\mathbf{M}}_{ij} \right)^2 \tag{19}$$

where n is the number of modes to be matched and $\overline{\mathbf{M}}$ is defined as shown in equation (20).

$$\overline{\mathbf{M}} = \Phi_G^T \mathbf{T}^T \mathbf{M} \mathbf{T} \Phi_G \tag{20}$$

In equation 20 above, the mass matrix $\mathbf{M}$ is calculated from the FE model, while the target eigen-matrix Φ_G is measured from the GVT. The eigen-matrix Φ_G remains constant during the optimization procedure. A transformation matrix $\mathbf{T}$ in the above equation is based on Guyan reduction, improved reduction system (ref. 14) or the system equivalent reduction expansion process (SEREP) (ref. 15). This reduction is required due to the limited number of available sensor locations and difficulties in measuring the rotational DOFs.

Step 3: Tuning Frequencies and Mode Shapes

Two different types of approach can be used for tuning the frequencies and mode shapes. In the first option, shown in equations (21) and (22), the objective function considered combines the normalized errors between GVT and computed frequencies with the total error associated with the off-diagonal terms of the orthonormalized stiffness matrix.

$$J_{12} = \sum_{i=1}^{n} \left(\frac{\Omega_i - \Omega_{iG}}{\Omega_i} \right)^2 \tag{21}$$

$$J_{13} = \sum_{i=1,\, j=1,\, i \neq j}^{n} \left(\overline{\mathbf{K}}_{ij} \right)^2 \tag{22}$$

The matrix $\overline{\mathbf{K}}$ is obtained from the matrix products as shown in equation (23):

$$\overline{\mathbf{K}} = \Phi_{\mathrm{G}}^T \mathbf{T}^T \mathbf{K} \mathbf{T} \Phi_{\mathrm{G}} \tag{23}$$

where the stiffness matrix, $\mathbf{K}$, is calculated from the FE model.

In the second option, shown in equations (24) and (25), the error norm combines the normalized error between the GVT and computed frequencies with the total error between the GVT and computed mode shapes at given sensor points.

$$J_{12} = \sum_{i=1}^{n} \left(\frac{\Omega_i - \Omega_{iG}}{\Omega_i} \right)^2 \tag{24}$$

$$J_{13} = \sum_{i=1}^{m} \sum_{j=1}^{n} \left(\Phi_{ij} - \Phi_{ijG} \right)^2 \tag{25}$$

In this study, the second option for tuning frequencies and mode shapes was employed since the definition of the objective function is much simpler than in the first option for this application. Any errors in both the modal frequencies and the mode shapes are minimized by including an index for each of these in the objective function. For this option, a small number of sensor locations can be used at which errors between the GVT and computed mode shapes are obtained. Any one of J_1 thru J_{13} can be used as the objective function with the others treated as constraints. This gives the flexibility to achieve the particular optimization goal while maintaining the other properties at as close to the desired target value as possible. The optimization problem statement can be written as:

Minimize J_i
Such that $J_k \leq \varepsilon_k$, for $k = 1$ thru 13 and $k \neq i$

where ε_k is a small value which can be adjusted according to the tolerance of each constraint condition.

TEST ARTICLE

The ATW2 was used to demonstrate NASA Dryden's MDAO tool through the process of ground vibration testing and the model tuning technique. This test article was a small-scale airplane wing comprised of an airfoil and wing tip boom as shown in figure 3, based on the ATW1 design. This wing was formulated based on a NACA-65A004 airfoil shape with a 3.28 aspect ratio. The wing had a half span of 18 in. with root chord length of 13.2 in. and tip chord length of 8.7 in. The total area of this wing was 197 in^2. The wing tip boom was a 1-in. diameter hollow tube of 21.5 in. length. The total weight of the wing was 2.66 lb.

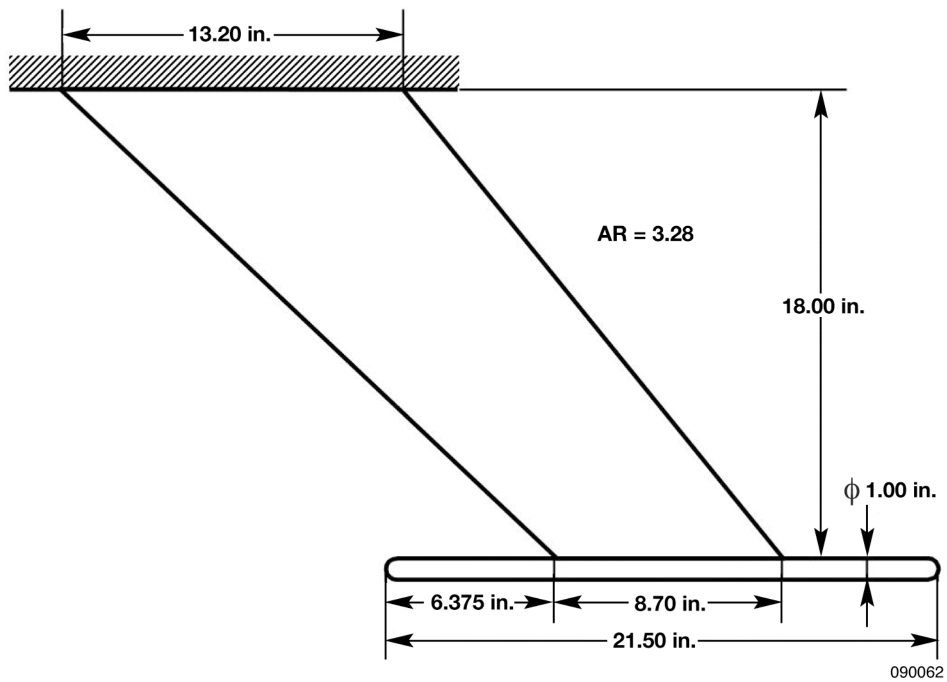

Figure 3. Dimension of the ATW2.

Since the ATW was attached to the F15B flight test fixture, the construction of the wing was limited to lightweight materials with no metal, due to safety concerns. The wing and spar were constructed from fiberglass cloth, the boom was constructed from carbon fiber composite, the wing core was constructed from rigid foam, and the components were attached by epoxy. The wing skin was made of three plies of fiberglass cloth, each about 0.01 in. thick. The internal spar located at the 30% chord line was composed of 10 plies, 0.05 in. thick of carbon at the root but decreases to 1 ply, 0.005 in. thick at the tip.

TEST SETUP

Ground vibration tests were performed to determine the dynamic modal characteristics of the ATW2. In the test set up, the ATW2 was clamped on to a circular plate, which was bolted to a mounting panel, and then installed into a small strong back called the ground test fixture in the NASA Dryden Flight Loads Laboratory. The PONTOS photogrammetry optical measuring system (Gesellschaft für Optische Messtechnik, Braunschweig, Germany), as shown in figure 4, was used to measure output displacement/acceleration at the sensor points. For the excitation method, an impact hammer with an impedance head was used to excite the ATW2's natural frequencies and mode shapes as well as to measure input forces.

090063

Figure 4. The PONTOS photogrammetry optical measuring system.

PONTOS is a non-contact optical 3D measuring system. It analyzes, computes, and documents object deformations, rigid body movements, and the dynamic behavior of a measuring point (ref. 16). The PONTOS system provides an alternative for complex sensor technology like laser sensor, draw-wire sensors or accelerometers, which are commonly used in GVTs for measuring responses of the structure. The features of the PONTOS system include:

- Unlimited number of sensors. The sensor markers are weightless, and a large number of sensors can be used at the same time without altering the total weight or the mode shapes of the structure.
- Non-contact acquisition of the precise 3D position of any number of measuring points.
- Mobility and flexibility due to an easy and compact measuring system.
- Easy and quick adaptation to different measuring volumes and measuring tasks.

The limitations of the PONTOS system include:

- Measuring structural vibration up to 250 Hz.
- Measuring frame rate up to 500 Hz at 1280x1024 pixels.
- Measuring volume up to 1700x1360x1360 mm^3.
- Applying the sensors on a plane or slightly curved surface.

SENSOR PLACEMENT DISCUSSION

Only a small number of sensors were placed on the wing for the GVT compared to the full FE model DOFs. The selection of sensor locations were based on the sensor placement algorithms previously discussed in Section II. In order to compare different sensor placement algorithms, the determinant of **FIM** was calculated for different sets of sensor locations. Results are summarized in table 1 and the corresponding sensor locations are shown in figure 5.

Table 1. Comparison of the determinant of FIM for different sensor placement algorithm.

Sensor placement algorithms	det(FIM) (30 sensors, 3 modes)
Effective independence	753.1
Genetic algorithm*	753.1
Kinetic energy	303.6
Iterative Guyan reduction	59.5
Non-iterative Guyan reduction	8.6
Model configuration (25 sensors)	50.0
Driving point residue	97.0

* Based on 150 populations and 500 generations

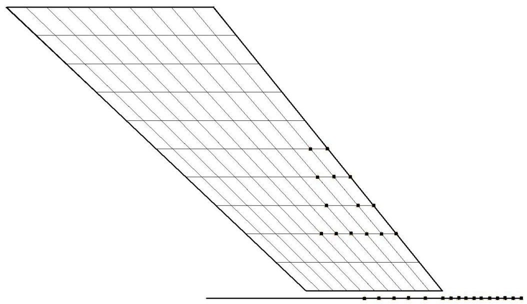

Figure 5a. DPR method.

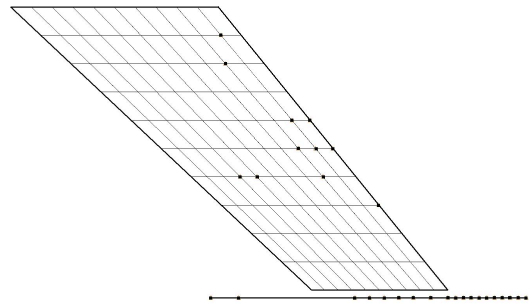

Figure 5b. KE method.

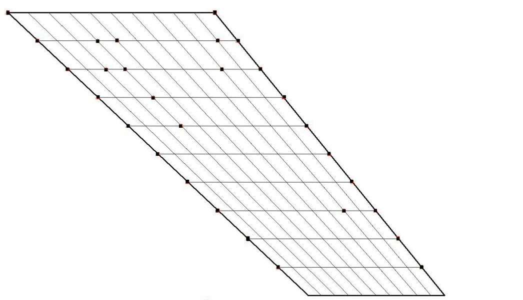

Figure 5c. Guyan reduction method.

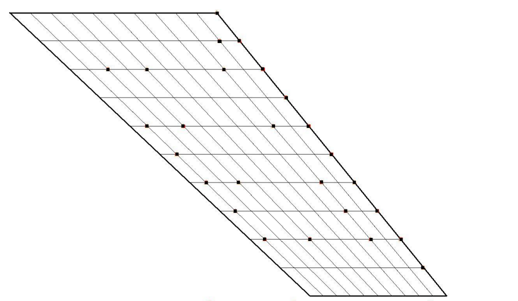

Figure 5d. Iterative Guyan reduction method.

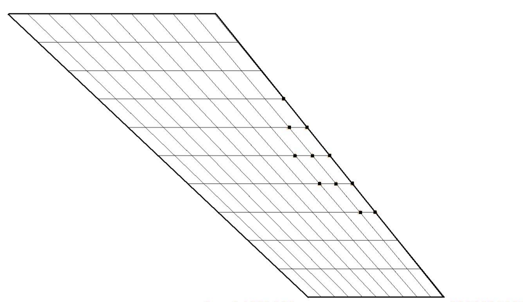

Figure 5e. Effective independence method.

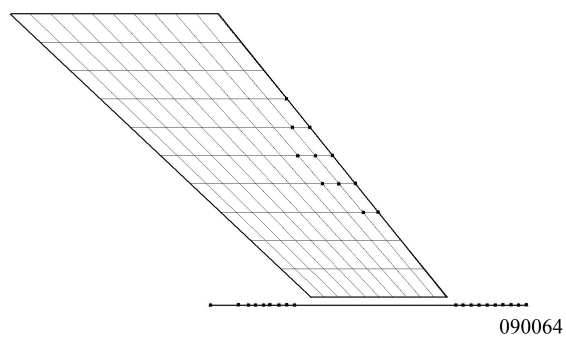

Figure 5f. Genetic algorithm.

Figure 5. Sensor locations from different sensor placement algorithms.

In table 1, the EI and GA methods have the same determinant of **FIM** value. This is due to the fact that the EI method is also an optimization process. In this application, both the EI and GA methods found the globally optimal value. The sensor locations with higher determent of **FIM** value were used for the GVT response measurement locations.

For the excitation point selection, the weighted maximum driving point residue method was used to determine the excitation locations. The predicted sensor locations and excitation point based on the FE model of the ATW2 is shown in figure 6 and the corresponding coordinates are given in table 2.

At the time of this ATW2 research work, only the GVT results with the sensor placements based on the model configuration were available. Therefore, these data were used for the FE model tuning process.

The sensor locations and excitation point of this GVT are shown in figure 7, and its coordinates are listed in table 3. Figure 8 shows the typical time history and frequency response curves of the ATW2 ground vibration tests.

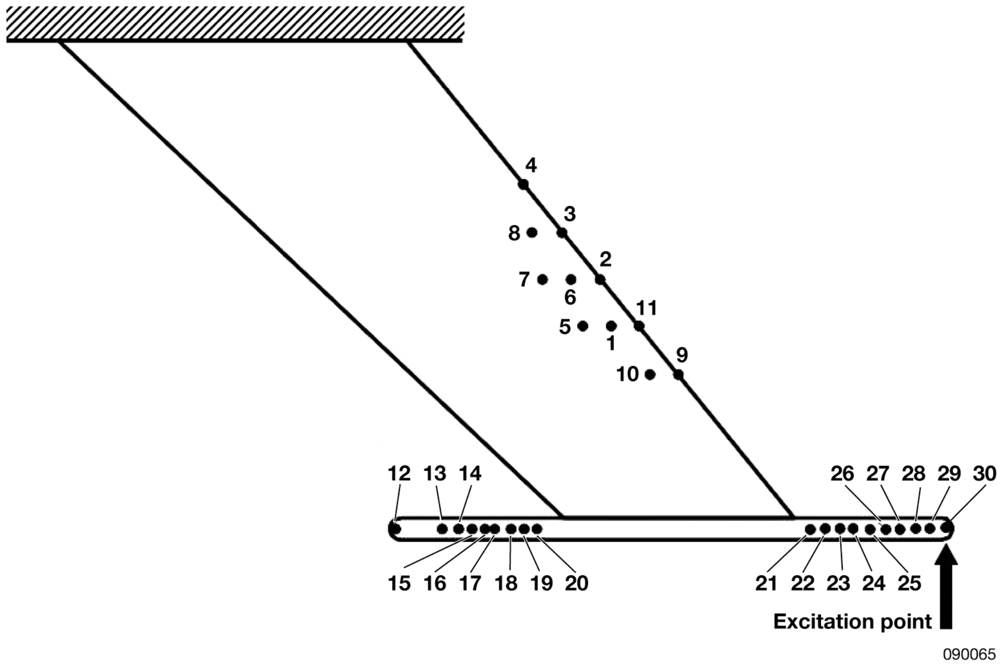

Figure 6. Predicted sensor/excitation locations.

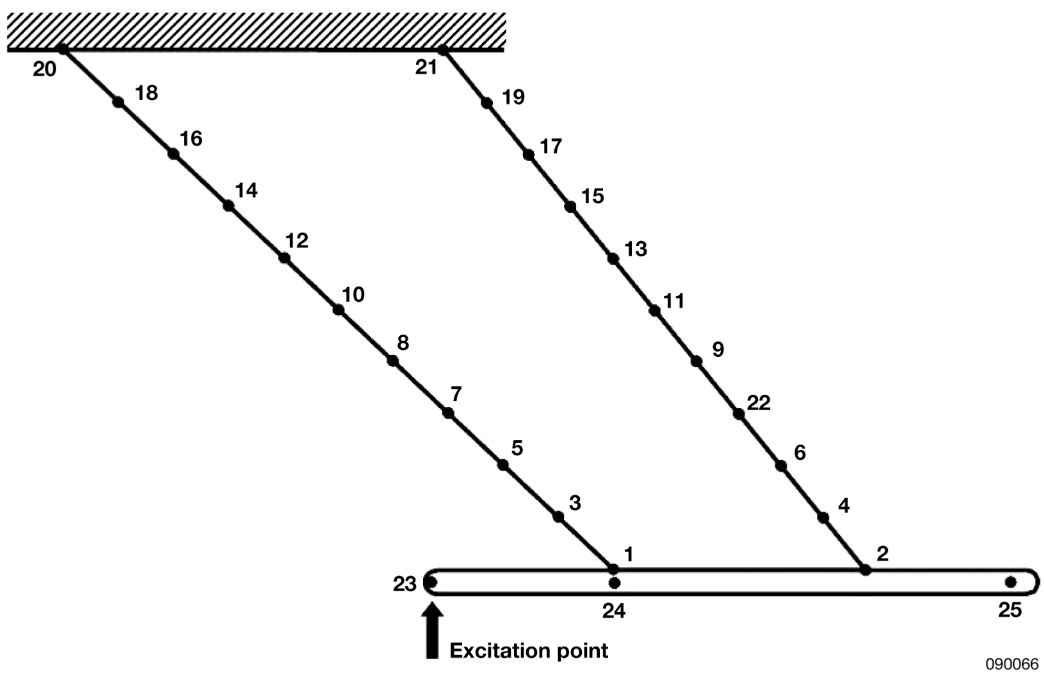

Figure 7. GVT sensor/excitation locations.

Table 2. Sensor locations for Figure 6.

Sensor point	Coordinates (inch)		
	X	Y	Z
1	20.9244	-10.80	-0.05
2	21.9750	-10.80	0
3	19.0499	-7.20	0
4	17.5875	-5.40	-0.001
5	19.8735	-10.80	0.1016
6	19.4167	-9.00	0.0537
7	18.3209	-9.00	0.1059
8	17.9092	-7.20	0.0559
9	23.4375	-12.60	0
10	22.4317	-12.60	0.0493
11	21.9750	-10.80	0
12	12.7500	-18.50	0
13	14.5000	-18.50	0
14	15.1250	-18.50	0
15	15.6250	-18.50	0
16	16.1250	-18.50	0
17	16.5000	-18.50	0
18	17.1250	-18.50	0
19	17.6250	-18.50	0
20	18.1250	-18.50	0
21	28.3250	-18.50	0
22	28.8250	-18.50	0
23	29.3250	-18.50	0
24	29.8250	-18.50	0
25	30.3250	-18.50	0
26	30.8250	-18.50	0
27	31.3250	-18.50	0
28	31.8250	-18.50	0
29	32.3250	-18.50	0
30	32.8250	-18.50	0

Table 3. Sensor locations for Figure 7.

Sensor point	Coordinates (inch)		
	X	Y	Z
1	19.125	-18.00	0
2	27.825	-18.00	0
3	17.212	-16.20	0
4	26.362	-16.20	0
5	15.300	-14.40	0
6	24.900	-14.40	0
7	13.387	-12.56	0
8	11.475	-10.80	0
9	21.975	-10.80	0
10	9.5625	-9.00	0
11	20.5125	-9.0	0
12	7.65	-7.2	0
13	19.0499	-7.2	0
14	5.7375	-5.4	0
15	17.5875	-5.4	0
16	3.825	-3.6	0
17	16.125	-3.6	0
18	1.9125	-1.8	0
19	14.6625	-1.8	0
20	0	0	0
21	13.2	0	0
22	23.4375	-12.6	0
23	12.75	-18.5	0
24	19.125	-18.5	0
25	32.825	-18.5	0

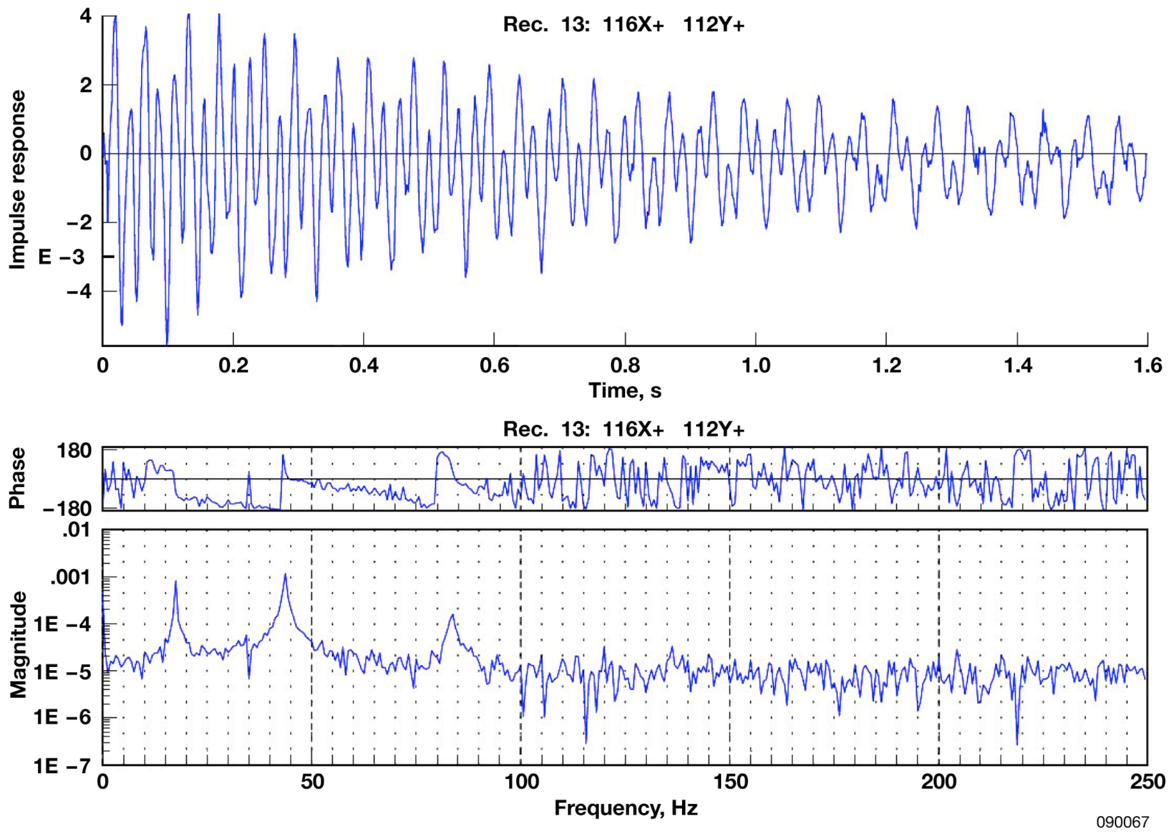

Figure 8. Typical time history and frequency response GVT results for the ATW2.

MODEL TUNING

The frequencies and mode shapes of first bending, first torsion and second bending modes; and total mass from the GVT are listed in table 4. The measurements of table 4 were based on the time history responses data collected by the PONTOS system at each of the sensor points. The eigensystem realization algorithm routine, which was developed by Juang and Pappa (ref. 17) at NASA Langley Research Center (Hampton, Virginia), was then used to identify the frequencies and mode shapes of the system.

Table 4. Measured frequencies and mode shapes (Z direction).

Sensor point	Mode 1 (17.24 Hz)	Mode 2 (44.10 Hz)	Mode 3 (84.00 Hz)
1	0.481	-0.398	-0.325
2	0.755	0.409	-0.187
3	0.386	-0.390	-0.149
4	0.670	0.353	0.142
5	0.311	-0.408	0.088
6	0.589	0.254	0.455
7	0.214	-0.320	0.113
8	0.139	-0.252	0.157
9	0.368	0.082	0.912
10	0.085	-0.177	0.131
11	0.281	0.036	1.000
12	0.047	-0.116	0.140
13	0.196	0.021	0.917
14	0.018	-0.067	0.053
15	0.157	0.018	0.870
16	0.006	0.022	-0.012
17	0.081	0.026	0.587
18	0.008	0.007	0.006
19	0.035	0.025	0.345
20	0.010	0.008	0.017
21	0.014	0.022	0.125
22	0.451	-0.111	0.765
23	0.312	-1.000	-0.582
24	0.518	-0.432	-0.523
25	1.000	0.962	-0.196

Corresponding numerical FE model frequencies and mode shapes computed using MSC/NASTRAN (MSC. Software Corporation, Santa Ana, California) (ref. 18) are shown in figure 9. The FE model in the MSC/NASTRAN format is provided in the appendix. The frequency differences between the GVT and the numerical results before model tuning (shown in table 5) were 53% in the second mode and 12% in the third mode, both of which greatly exceed the 3% limitation for the primary modes allowed by military specifications (refs. 19, 20). Therefore, the FE model needs to be updated for a more reliable flutter analysis.

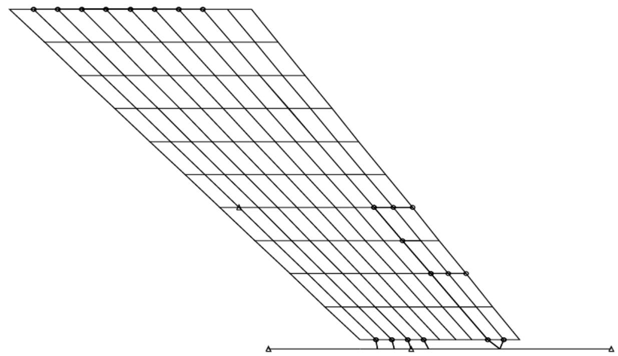

Figure 9a. MSC/NASTRAN FE model.

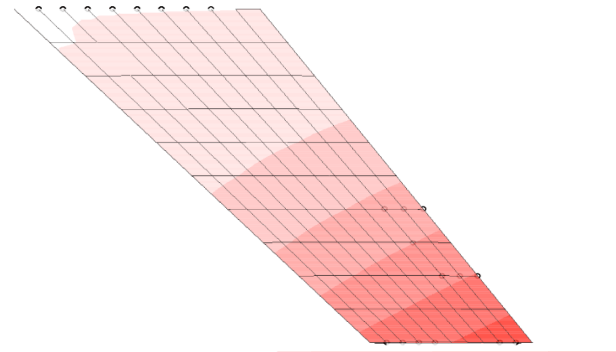

Figure 9b. Mode 1 (1st bending): 17.7048 Hz.

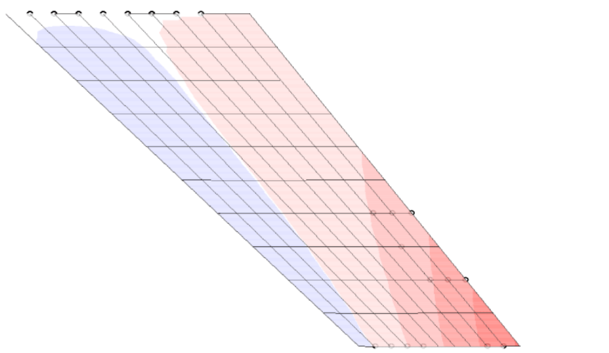

Figure 9c. Mode 2 (1st torsion): 20.9207 Hz.

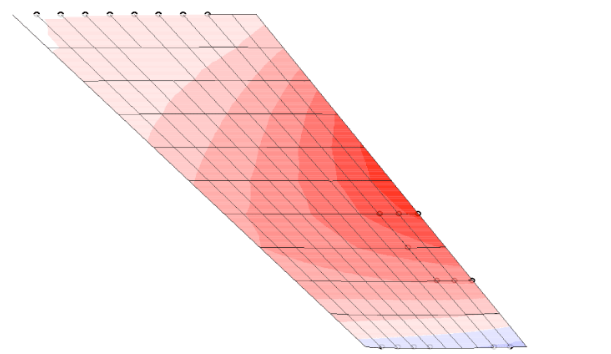

090068

Figure 9d. Mode 3 (2nd bending): 88.3203 Hz.

Figure 9. Finite element model and mode shapes before tuning.

Table 5. Frequencies and total weight of the ATW2 before and after model tuning.

	GVT (Hz)	Before		After	
		MSC/NASTRAN (Guyan/Full; Hz)	Error (%)	MSC/NASTRAN (SEREP/Full; Hz)	Error (%)
Mode 1	17.24	17.71/17.70	2.72/2.68	17.79/17.79	3.19/3.19
Mode 2	44.10	20.93/20.92	-52.5/-52.6	44.71/44.71	1.38/1.38
Mode 3	84.00	93.91/88.32	11.80/5.14	84.33/84.33	0.39/0.39
Total weight (lb)	2.66	2.77	4.13	2.72	2.25

Since Guyan reduction is a static condensation, it is only accurate for lower modes. For higher modes, the errors become too large as shown in table 5. Unlike the Guyan reduction, the SEREP process preserves the dynamic character of the original full system model for selected modes of interest. Therefore the dynamic characteristics of the reduced model were virtually the same as the full model shown in table 5. Therefore, the SEREP model reduction process was used in this ATW2 model update application.

Using frequency difference as an objective function; and mass properties, mass orthogonality, and mode shapes as constraint equations; the frequencies before and after model tuning are presented in table

5. Dramatic improvement was noted, in that after model tuning, the frequencies difference was reduced to 1.38% in the second mode and 0.39% in the third mode.

Table 6 shows the center of gravity, moment of inertia, orthonormalized mass matrix, and modal assurance criterion (MAC) values of the ATW2 before and after model tuning. The off-diagonal terms of the orthonormalized mass matrix, maximum of 37% before model tuning, were minimized in the second tuning step. The maximum off-diagonal term of 7.4% after model tuning is observed in table 6, and this off-diagonal term of the orthonormalized mass matrix satisfies the 10% limitation allowed by military specifications. Model correlation with the test data prior to model tuning was poor and unacceptable to proceed with flight. The MAC values of 0.52 and 0.73 for modes 2 and 3 before model tuning become 0.97 and 0.95, respectively. Therefore, we can conclude that excellent model correlation with the test data was achieved after model tuning, which lead to a more reliable flutter speed prediction.

Table 6. Summary of center of gravity, moment of inertia, orthonormalized mass matrix and MAC values for the ATW2 before and after model tuning.

			Before tuning			After tuning		
C.G. (X,Y,Z)			14.22, -11.86, -0.011			13.089, -7.61, -0.0080		
Ixx			73.44			97.52		
Iyy			74.74			118.13		
Izz			148.1			215.5		
Ixy			-43.03			-85.55		
Ixz			0.032			0.0286		
Iyz			-0.02			0.0956		
Orthonormalized mass matrix			1	2	3	1	2	3
		1	1	25.0%	4.6%	1	4.0%	-5.7%
		2	0.2467	1	37.0%	0.0395	1	-7.4%
		3	0.0463	0.3681	1	-0.0565	-0.0743	1
MAC	Mode 1		0.90			0.99		
	Mode 2		0.52			0.97		
	Mode 3		0.73			0.95		

CONCLUDING REMARKS

This paper describes the ground vibration test (GVT) and model tuning procedures for the second aerostructures test wing (ATW2), which was developed at the National Aeronautics and Space Administration Dryden Flight Research Center (Edwards, California) for demonstrating flutter and advanced aeroelastic test techniques. In the sensor locations selection process, it was found that the effective independence (EI) and the genetic algorithm (GA) gave a higher determinant value of the Fisher information matrix (**FIM**) and thus, should be used for determining the sensor locations.

The finite element (FE) model tuning process was a challenging task, which depended not only on the accuracy of the experimental data, but also required a good prediction of the design variables for the optimization. After tuning the FE model, the frequency differences between GVT and the numerical results were within 3%, and the off-diagonal terms of the orthonormalized mass matrix were within 10%, both of which satisfy the military specifications. Excellent mode shape correlations were also achieved through the high modal assurance criterion (MAC) value (greater than 95%). With the updated FE model, the accuracy of flutter analysis can be improved and the flutter boundary prediction will be more reliable.

REFERENCES

1. Lind, Rick, David Voracek, Roger Truax, Tim Doyle, Starr Potter, and Marty Brenner, "A Flight Test to Demonstrate Flutter and Evaluate the Flutterometer," *The Aeronautical Journal*, Vol. 107, No. 1076, pp. 577 – 588, October 2003.

2. Pak, Chan-gi, and Wesley Li, "Multidisciplinary Design, Analysis, and Optimization Tool Development Using a Genetic Algorithm," *Proceedings of the 26th Congress of International Council of the Aeronautical Science*, Anchorage, 2008.

3. Kammer, Daniel C., "Sensor Placement for On-Orbit Modal Identification and Correlation of Large Space Structures," *AIAA Journal of Guidance, Control and Dynamics*, Vol. 14, No. 2, pp. 251-259, 1991.

4. Charbonneau, Paul, and Barry Knapp, *A User's Guide to PIKAIA 1.0*, National Center for Atmospheric Research, Boulder, CO, 1995.

5. Friswell, M. I., and J. E. Mottershead, *Finite Element Model Updating in Structural Dynamics*, Kluwer Academic Publishers, Dordrecht, 1995.

6. Guyan, Robert J., "Reduction of Stiffness and Mass Matrices," *AIAA Journal*, Vol. 3, No. 2, p. 380, 1965.

7. Tinker, Michael L., "Accelerometer Placement for the International Space Station Node Modal Test," AIAA-1998-2078, *AIAA/ASME/ASCE/AHS/ASC Structures, Structural Dynamics, and Materials Conference and Exhibit, 39th and AIAA/ASME/AHS Adaptive Structures Forum*, Long Beach, CA, April 20-23, 1998.

8. EI-Borgi, S., M. Neifar, F. Cherif, S. Choura, and H. Smaoui, "Modal Identification, Model Updating and Nonlinear Analysis of a Reinforced Concrete Bridge," *Journal of Vibration and Control*, Vol. 14, No. 4, pp. 511-530, 2008.

9. Pak, Chan-gi, "Finite Element Model Tuning Using Measured Mass Properties and Ground Vibration Test Data," *ASME Journal of Vibration and Acoustics*, Vol. 131, No. 1, February 2009.

10. Lung, Shun-fat, and Chan-gi Pak, "Structural Model Tuning Capability in an Object-Oriented Multidisciplinary Design, Analysis, and Optimization Tool," *Proceedings of the 26th Congress of International Council of the Aeronautical Sciences*, Anchorage, 2008.

11. Herrera, Claudia Y., and Chan-gi Pak, "Build-up Approach to Updating the Mock Quiet Spike Beam Model," AIAA-2007-1776, *Proceedings of the 48th AIAA/ASME/ASCE/AHS/ASC Structures, Structural Dynamics, and Materials Conference*, Honolulu, Hawaii, April 23-26, 2007.

12. Vanderplaats, Garret N., *Numerical Optimization Techniques for Engineering Design*, 3rd ed., Vanderplaats Research & Development, Inc. 2001.

13. Yeniay, Özgür, "Penalty Function Methods For Constrained Optimization Using Genetic Algorithms," *Mathematical and Computational Applications*, Vol. 10, No. 1, pp. 45-56, 2005.

14. O'Callahan, John C., "A New Procedure for an Improved Reduced System (IRS) Model," *Proceedings of the 7th International Modal Analysis Conference*, Vol. 1, pp. 17-21, Las Vegas, 1989.

15. O'Callahan, J. C., P. Avitabile, and R. Riemer, "System Equivalent Reduction Expansion Process," *Proceedings of the 7th International Modal Analysis Conference*, Vol. 1, pp. 29-37, Las Vegas, 1989.

16. *PONTOS User Manual Version 6.0*, Gesellschaft für Optische Messtechnik, Braunschweig, Germany, 2007.

17. Juang, Jer-Nan, and Richard S. Pappa, "An Eigensystem Realization Algorithm for Modal Parameter Identification and Modal Reduction," *AIAA Journal of Guidance, Control, and Dynamics*, Vol. 8, No. 5, pp. 620-627, 1984.

18. MSC.Software Corporation, *MSC.Nastran 2005 Quick Reference Guide: Volume 1*, MSC.Software Corporation, 2005.

19. *Test Requirements for Launch, Upper-Stage, and Space Vehicles*, MIL-STD-1540C Section 6.2.10, September 15, 1994.

20. Norton, William J., *Structures Flight Test Handbook*, AFFTC-TIH-90-001, November 1990.

APPENDIX
THE FE MODEL IN THE MSC/NASTRAN FORMAT

```
$ NASTRAN input file created by the MSC MSC.Nastran input file
$ translator ( MSC.Patran 13.1.116 ) on December  13, 2007 at 08:05:41.
ASSIGN OUTPUT4='atw2c_maa.op4',UNIT=30,STATUS=UNKNOWN,FORM=FORMATTED
ASSIGN OUTPUT4='atw2c_kaa.op4',UNIT=31,STATUS=UNKNOWN,FORM=FORMATTED
SOL 103
$ Direct Text Input for Executive Control
$==============================
$ DMAP ALTER SOL 103
     COMPILE SEMODES SOUIN=MSCSOU LIST REF$
     ALTER 315$
     OUTPUT4 MAA///30/2//9$
     OUTPUT4 KAA///31/2//9$
     ENDALTER
$===============================
CEND
SEALL = ALL
SUPER = ALL
TITLE = ATW2
$ECHO = SORT
$ Direct Text Input for Global Case Control Data
SUBCASE 1
$ Subcase name : ATW2C
   SUBTITLE=ATW2C
   METHOD = 1
   SPC = 2
$   VECTOR(PLOT,SORT1,REAL)=ALL
   DISP=ALL
GPKE = ALL
BEGIN BULK
PARAM   POST    -1
PARAM   AUTOSPC YES
PARAM   WTMASS  .002588
PARAM   GRDPNT  0
PARAM   NOCOMPS,-1
PARAM,   USETPRT, 10
EIGRL    1                      10      0                       MAX
$ Direct Text Input for Bulk Data
$ Elements and Element Properties for region : pbar.700
PBAR     700     701    .5      .1      .1
$ Pset: "pbar.700" will be imported as: "pbar.700"
CBAR     300     700     303     308    -.061556-.998102.0018318
CBAR     301     700     9       124    -.061556-.998102.0018318
$ Elements and Element Properties for region : pcomp.500
$ Composite Property Record created from P3/PATRAN composite material
$ record : pcomp.500
$ Composite Material Description :
PCOMP    500    .01                               0.      0.
         501    .01     45.     YES     501    .01     -45.     YES
$ Pset: "pcomp.500" will be imported as: "pcomp.500"
CQUAD4   500     500     229     240     113     102     0.      0.
CQUAD4   501     500     218     229     102     91      0.      0.
```

```
CQUAD4   502     500     207     218     91      80      0.      0.
CQUAD4   503     500     196     207     80      69      0.      0.
CQUAD4   504     500     185     196     69      58      0.      0.
CQUAD4   505     500     174     185     58      47      0.      0.
CQUAD4   506     500     163     174     47      36      0.      0.
CQUAD4   507     500     152     163     36      25      0.      0.
CQUAD4   508     500     141     152     25      14      0.      0.
CQUAD4   509     500     130     141     14      3       0.      0.
CQUAD4   510     500     227     104     115     238     0.      0.
CQUAD4   511     500     216     93      104     227     0.      0.
CQUAD4   512     500     205     82      93      216     0.      0.
CQUAD4   513     500     194     71      82      205     0.      0.
CQUAD4   514     500     183     60      71      194     0.      0.
CQUAD4   515     500     172     49      60      183     0.      0.
CQUAD4   516     500     161     38      49      172     0.      0.
CQUAD4   517     500     150     27      38      161     0.      0.
CQUAD4   518     500     139     16      27      150     0.      0.
CQUAD4   519     500     128     5       16      139     0.      0.
$ Elements and Element Properties for region : celas2.ca6.cb6
PELAS    1      50.
$ Pset: "celas2.ca6.cb6" will be imported as: "pelas.1"
CELAS1   302     1       9       6       303     6
$ Elements and Element Properties for region : pelas.2
PELAS    2      1.+8
$ Pset: "pelas.2" will be imported as: "pelas.2"
CELAS1   4006    2       403     6       402     6
$ Elements and Element Properties for region : celas2.ca5.cb5
PELAS    3      1.+8
$ Pset: "celas2.ca5.cb5" will be imported as: "pelas.3"
CELAS1   4005    3       403     5       402     5
$ Elements and Element Properties for region : celas2.ca4.cb4
PELAS    4      1.+8
$ Pset: "celas2.ca4.cb4" will be imported as: "pelas.4"
CELAS1   4004    4       403     4       402     4
$ Elements and Element Properties for region : celas2.ca3.cb3
PELAS    5      1.+6
$ Pset: "celas2.ca3.cb3" will be imported as: "pelas.5"
CELAS1   4003    5       403     3       402     3
$ Elements and Element Properties for region : celas2.ca2.cb2
PELAS    6      1.+6
$ Pset: "celas2.ca2.cb2" will be imported as: "pelas.6"
CELAS1   4002    6       403     2       402     2
$ Elements and Element Properties for region : celas2.ca1.cb1
PELAS    7      1.+6
$ Pset: "celas2.ca1.cb1" will be imported as: "pelas.7"
CELAS1   4001    7       403     1       402     1
$ Elements and Element Properties for region : pshell.600
PSHELL   600     601     .03     601             601
$ Pset: "pshell.600" will be imported as: "pshell.600"
CTRIA3   600     600     241     111     112     0.      0.
CQUAD4   601     600     240     241     112     113     0.      0.
CQUAD4   602     600     239     240     113     114     0.      0.
CQUAD4   603     600     238     239     114     115     0.      0.
CQUAD4   604     600     237     238     115     116     0.      0.
CQUAD4   605     600     236     237     116     117     0.      0.
CQUAD4   606     600     235     236     117     118     0.      0.
CQUAD4   607     600     234     235     118     119     0.      0.
```

```
CQUAD4   608     600     233     234     119     120     0.      0.
CTRIA3   609     600     121     233     120     0.      0.
CTRIA3   610     600     219     89      90      0.      0.
CQUAD4   611     600     218     219     90      91      0.      0.
CQUAD4   612     600     217     218     91      92      0.      0.
CQUAD4   613     600     216     217     92      93      0.      0.
CQUAD4   614     600     215     216     93      94      0.      0.
CQUAD4   615     600     214     215     94      95      0.      0.
CQUAD4   616     600     213     214     95      96      0.      0.
CQUAD4   617     600     212     213     96      97      0.      0.
CQUAD4   618     600     211     212     97      98      0.      0.
CTRIA3   619     600     99      211     98      0.      0.
CTRIA3   620     600     197     67      68      0.      0.
CQUAD4   621     600     196     197     68      69      0.      0.
CQUAD4   622     600     195     196     69      70      0.      0.
CQUAD4   623     600     194     195     70      71      0.      0.
CQUAD4   624     600     193     194     71      72      0.      0.
CQUAD4   625     600     192     193     72      73      0.      0.
CQUAD4   626     600     191     192     73      74      0.      0.
CQUAD4   627     600     190     191     74      75      0.      0.
CQUAD4   628     600     189     190     75      76      0.      0.
CTRIA3   629     600     77      189     76      0.      0.
CTRIA3   630     600     175     45      46      0.      0.
CQUAD4   631     600     174     175     46      47      0.      0.
CQUAD4   632     600     173     174     47      48      0.      0.
CQUAD4   633     600     172     173     48      49      0.      0.
CQUAD4   634     600     171     172     49      50      0.      0.
CQUAD4   635     600     170     171     50      51      0.      0.
CQUAD4   636     600     169     170     51      52      0.      0.
CQUAD4   637     600     168     169     52      53      0.      0.
CQUAD4   638     600     310     311     305     306     0.      0.
CTRIA3   639     600     307     310     306     0.      0.
CTRIA3   640     600     153     23      24      0.      0.
CQUAD4   641     600     152     153     24      25      0.      0.
CQUAD4   642     600     151     152     25      26      0.      0.
CQUAD4   643     600     150     151     26      27      0.      0.
CQUAD4   644     600     149     150     27      28      0.      0.
CQUAD4   645     600     148     149     28      29      0.      0.
CQUAD4   646     600     147     148     29      30      0.      0.
CQUAD4   647     600     146     147     30      31      0.      0.
CQUAD4   648     600     314     308     303     313     0.      0.
CTRIA3   649     600     312     314     313     0.      0.
CTRIA3   650     600     131     1       2       0.      0.
CQUAD4   651     600     130     131     2       3       0.      0.
CQUAD4   652     600     129     130     3       4       0.      0.
CQUAD4   653     600     128     129     4       5       0.      0.
CQUAD4   654     600     127     128     5       6       0.      0.
CQUAD4   655     600     126     127     6       7       0.      0.
CQUAD4   656     600     125     126     7       8       0.      0.
CQUAD4   657     600     124     125     8       9       0.      0.
CQUAD4   658     600     123     124     9       10      0.      0.
CTRIA3   659     600     11      123     10      0.      0.
CQUAD4   660     600     145     146     31      32      0.      0.
CTRIA3   661     600     33      145     32      0.      0.
CQUAD4   662     600     167     168     53      54      0.      0.
CTRIA3   663     600     55      167     54      0.      0.
$ Elements and Element Properties for region : pshell.608
```

```
PSHELL   608     601     .06     601             601
$ Pset: "pshell.608" will be imported as: "pshell.608"
CQUAD4   700     608     309     311     305     304     0.      0.
CQUAD4   701     608     308     309     304     303     0.      0.
CQUAD4   702     608     31      42      157     146     0.      0.
CQUAD4   703     608     42      53      168     157     0.      0.
$ Elements and Element Properties for region : psolid.300
PSOLID   300     301     0
$ Pset: "psolid.300" will be imported as: "psolid.300"
CHEXA    200     300     13      2       3       14      142     131
         130     141
CHEXA    201     300     14      3       4       15      141     130
         129     140
CHEXA    202     300     24      13      14      25      153     142
         141     152
CHEXA    203     300     15      4       5       16      140     129
         128     139
CHEXA    204     300     25      14      15      26      152     141
         140     151
CHEXA    205     300     35      24      25      36      164     153
         152     163
CHEXA    206     300     16      5       6       17      139     128
         127     138
CHEXA    207     300     26      15      16      27      151     140
         139     150
CHEXA    208     300     36      25      26      37      163     152
         151     162
CHEXA    209     300     46      35      36      47      175     164
         163     174
CHEXA    210     300     17      6       7       18      138     127
         126     137
CHEXA    211     300     27      16      17      28      150     139
         138     149
CHEXA    212     300     37      26      27      38      162     151
         150     161
CHEXA    213     300     47      36      37      48      174     163
         162     173
CHEXA    214     300     57      46      47      58      186     175
         174     185
CHEXA    215     300     18      7       8       19      137     126
         125     136
CHEXA    216     300     28      17      18      29      149     138
         137     148
CHEXA    217     300     38      27      28      39      161     150
         149     160
CHEXA    218     300     48      37      38      49      173     162
         161     172
CHEXA    219     300     58      47      48      59      185     174
         173     184
CHEXA    220     300     68      57      58      69      197     186
         185     196
CHEXA    221     300     19      8       9       20      136     125
         124     135
CHEXA    222     300     29      18      19      30      148     137
         136     147
CHEXA    223     300     39      28      29      40      160     149
         148     159
```

CHEXA	224	300	49	38	39	50	172	161
	160	171						
CHEXA	225	300	59	48	49	60	184	173
	172	183						
CHEXA	226	300	69	58	59	70	196	185
	184	195						
CHEXA	227	300	79	68	69	80	208	197
	196	207						
CHEXA	228	300	20	9	10	21	135	124
	123	134						
CHEXA	229	300	30	19	20	31	147	136
	135	146						
CHEXA	230	300	40	29	30	41	159	148
	147	158						
CHEXA	231	300	50	39	40	51	171	160
	159	170						
CHEXA	232	300	60	49	50	61	183	172
	171	182						
CHEXA	233	300	70	59	60	71	195	184
	183	194						
CHEXA	234	300	80	69	70	81	207	196
	195	206						
CHEXA	235	300	90	79	80	91	219	208
	207	218						
CHEXA	236	300	31	20	21	32	146	135
	134	145						
CHEXA	237	300	41	30	31	42	158	147
	146	157						
CHEXA	238	300	51	40	41	52	170	159
	158	169						
CHEXA	239	300	61	50	51	62	182	171
	170	181						
CHEXA	240	300	71	60	61	72	194	183
	182	193						
CHEXA	241	300	81	70	71	82	206	195
	194	205						
CHEXA	242	300	91	80	81	92	218	207
	206	217						
CHEXA	243	300	101	90	91	102	230	219
	218	229						
CHEXA	244	300	304	303	313	300	309	308
	314	302						
CHEXA	245	300	52	41	42	53	169	158
	157	168						
CHEXA	246	300	62	51	52	63	181	170
	169	180						
CHEXA	247	300	72	61	62	73	193	182
	181	192						
CHEXA	248	300	82	71	72	83	205	194
	193	204						
CHEXA	249	300	92	81	82	93	217	206
	205	216						
CHEXA	250	300	102	91	92	103	229	218
	217	228						
CHEXA	251	300	112	101	102	113	241	230
	229	240						
CHEXA	252	300	305	304	300	306	311	309

	302	310						
CHEXA	253	300	63	52	53	64	180	169
	168	179						
CHEXA	254	300	73	62	63	74	192	181
	180	191						
CHEXA	255	300	83	72	73	84	204	193
	192	203						
CHEXA	256	300	93	82	83	94	216	205
	204	215						
CHEXA	257	300	103	92	93	104	228	217
	216	227						
CHEXA	258	300	113	102	103	114	240	229
	228	239						
CHEXA	259	300	64	53	54	65	179	168
	167	178						
CHEXA	260	300	74	63	64	75	191	180
	179	190						
CHEXA	261	300	84	73	74	85	203	192
	191	202						
CHEXA	262	300	94	83	84	95	215	204
	203	214						
CHEXA	263	300	104	93	94	105	227	216
	215	226						
CHEXA	264	300	114	103	104	115	239	228
	227	238						
CHEXA	265	300	75	64	65	76	190	179
	178	189						
CHEXA	266	300	85	74	75	86	202	191
	190	201						
CHEXA	267	300	95	84	85	96	214	203
	202	213						
CHEXA	268	300	105	94	95	106	226	215
	214	225						
CHEXA	269	300	115	104	105	116	238	227
	226	237						
CHEXA	270	300	86	75	76	87	201	190
	189	200						
CHEXA	271	300	96	85	86	97	213	202
	201	212						
CHEXA	272	300	106	95	96	107	225	214
	213	224						
CHEXA	273	300	116	105	106	117	237	226
	225	236						
CHEXA	274	300	97	86	87	98	212	201
	200	211						
CHEXA	275	300	107	96	97	108	224	213
	212	223						
CHEXA	276	300	117	106	107	118	236	225
	224	235						
CHEXA	277	300	108	97	98	109	223	212
	211	222						
CHEXA	278	300	118	107	108	119	235	224
	223	234						
CHEXA	279	300	119	108	109	120	234	223
	222	233						
CPENTA	280	300	2	1	131	13	12	142
CPENTA	281	300	13	12	142	24	23	153

```
CPENTA   282     300     24      23      153     35      34      164
CPENTA   283     300     35      34      164     46      45      175
CPENTA   284     300     46      45      175     57      56      186
CPENTA   285     300     57      56      186     68      67      197
CPENTA   286     300     68      67      197     79      78      208
CPENTA   287     300     79      78      208     90      89      219
CPENTA   288     300     90      89      219     101     100     230
CPENTA   289     300     21      22      134     10      11      123
CPENTA   290     300     101     100     230     112     111     241
CPENTA   291     300     32      33      145     21      22      134
CPENTA   292     300     300     301     302     313     312     314
CPENTA   293     300     306     307     310     300     301     302
CPENTA   294     300     65      66      178     54      55      167
CPENTA   295     300     76      77      189     65      66      178
CPENTA   296     300     87      88      200     76      77      189
CPENTA   297     300     98      99      211     87      88      200
CPENTA   298     300     109     110     222     98      99      211
CPENTA   299     300     120     121     233     109     110     222
$ Elements and Element Properties for region : conm2
CONM2    400     500     0       0.475   0.      0.      0.
         0.      0.      0.      0.      0.      0.
CONM2    401     513     0       0.      0.      0.      0.
         0.      0.      0.      0.      0.      0.
CONM2    402     529     0       0.075   0.      0.      0.
         0.      0.      0.      0.      0.      0.
CONM2    406     68      0       0.03    0.      0.      0.
         0.      0.      0.      0.      0.      0.
CONM2    407     57      0       0.03    0.      0.      0.
         0.      0.      0.      0.      0.      0.
CONM2    408     46      0       0.03    0.      0.      0.
         0.      0.      0.      0.      0.      0.
CONM2    409     35      0       0.03    0.      0.      0.
         0.      0.      0.      0.      0.      0.
CONM2    410     24      0       0.03    0.      0.      0.
         0.      0.      0.      0.      0.      0.
CONM2    412     91      0       0.0638  0.      0.      0.
         0.      0.      0.      0.      0.      0.
CONM2    413     97      0       0.0638  0.      0.      0.
         0.      0.      0.      0.      0.      0.
CONM2    414     103     0       0.0638  0.      0.      0.
         0.      0.      0.      0.      0.      0.
CONM2    415     109     0       0.0638  0.      0.      0.
         0.      0.      0.      0.      0.      0.
CONM2    416     212     0       0.0638  0.      0.      0.
         0.      0.      0.      0.      0.      0.
CONM2    417     218     0       0.0638  0.      0.      0.
         0.      0.      0.      0.      0.      0.
CONM2    418     228     0       0.0638  0.      0.      0.
         0.      0.      0.      0.      0.      0.
CONM2    419     222     0       0.0638  0.      0.      0.
         0.      0.      0.      0.      0.      0.
$ Elements and Element Properties for region : pbar.39
PBAR     39      901     .097314 .011411 .011411 .022821
        .5                      .5      -.5                             -.5
$ Pset: "pbar.39" will be imported as: "pbar.39"
CBAR     800     39      501     500     0.     -1.      0.
CBAR     801     39      502     501     0.     -1.      0.
```

```
CBAR     802     39      503     502     0.      -1.      0.
CBAR     803     39      504     503     0.      -1.      0.
CBAR     804     39      505     504     0.      -1.      0.
CBAR     805     39      506     505     0.      -1.      0.
CBAR     806     39      507     506     0.      -1.      0.
CBAR     807     39      508     507     0.      -1.      0.
CBAR     808     39      509     508     0.      -1.      0.
CBAR     809     39      510     509     0.      -1.      0.
CBAR     810     39      512     511     0.      1.       0.
CBAR     811     39      513     512     0.      1.       0.
CBAR     812     39      514     513     0.      1.       0.
CBAR     813     39      515     514     0.      -1.      0.
CBAR     814     39      516     515     0.      -1.      0.
CBAR     815     39      517     516     0.      -1.      0.
CBAR     816     39      518     517     0.      1.       0.
CBAR     817     39      519     518     0.      -1.      0.
CBAR     818     39      520     519     0.      -1.      0.
CBAR     819     39      521     520     0.      -1.      0.
CBAR     820     39      522     521     0.      -1.      0.
CBAR     821     39      523     522     0.      -1.      0.
CBAR     822     39      524     523     0.      -1.      0.
CBAR     823     39      525     524     0.      -1.      0.
CBAR     824     39      526     525     0.      -1.      0.
CBAR     825     39      527     526     0.      -1.      0.
CBAR     826     39      528     527     0.      -1.      0.
CBAR     827     39      529     528     0.      -1.      0.
CBAR     828     39      530     510     0.      -1.      0.
CBAR     829     39      511     530     0.      1.       0.
$ Elements and Element Properties for region : pcomp.41
$ Composite Property Record created from P3/PATRAN composite material
$ record : pcomp.10
$ Composite Material Description :
PCOMP    41      -.13            8000.   HOFF    0.      0.
         201     .11     0.      YES     202     .02     45.     YES
$ Pset: "pcomp.41" will be imported as: "pcomp.41"
CQUAD4   1002    41      228     239     240     229     4       0.
CQUAD4   1003    41      227     238     239     228     4       0.
CQUAD4   1012    41      217     228     229     218     4       0.
CQUAD4   1013    41      216     227     228     217     4       0.
CQUAD4   1202    41      102     113     114     103     4       0.
CQUAD4   1203    41      103     114     115     104     4       0.
CQUAD4   1212    41      91      102     103     92      4       0.
CQUAD4   1213    41      92      103     104     93      4       0.
$ Elements and Element Properties for region : pcomp.42
$ Composite Property Record created from P3/PATRAN composite material
$ record : pcomp.20
$ Composite Material Description :
PCOMP    42      -.09            8000.   HOFF    0.      0.
         201     .075    0.      YES     202     .015    45.     YES
$ Pset: "pcomp.42" will be imported as: "pcomp.42"
CQUAD4   1022    42      206     217     218     207     4       0.
CQUAD4   1023    42      205     216     217     206     4       0.
CQUAD4   1032    42      195     206     207     196     4       0.
CQUAD4   1033    42      194     205     206     195     4       0.
CQUAD4   1222    42      80      91      92      81      4       0.
CQUAD4   1223    42      81      92      93      82      4       0.
CQUAD4   1232    42      69      80      81      70      4       0.
```

```
CQUAD4   1233    42      70      81      82      71      4       0.
$ Elements and Element Properties for region : pcomp.43
$ Composite Property Record created from P3/PATRAN composite material
$ record : pcomp.30
$ Composite Material Description :
PCOMP    43      -.073           8000.   HOFF    0.      0.
         201     .058    0.      YES     202     .015    45.     YES
$ Pset: "pcomp.43" will be imported as: "pcomp.43"
CQUAD4   1042    43      184     195     196     185     4       0.
CQUAD4   1043    43      183     194     195     184     4       0.
CQUAD4   1052    43      173     184     185     174     4       0.
CQUAD4   1053    43      172     183     184     173     4       0.
CQUAD4   1242    43      58      69      70      59      4       0.
CQUAD4   1243    43      59      70      71      60      4       0.
CQUAD4   1252    43      47      58      59      48      4       0.
CQUAD4   1253    43      48      59      60      49      4       0.
$ Elements and Element Properties for region : pcomp.44
$ Composite Property Record created from P3/PATRAN composite material
$ record : pcomp.40
$ Composite Material Description :
PCOMP    44      -.038           8000.   HOFF    0.      0.
         201     .023    0.      YES     202     .015    45.     YES
$ Pset: "pcomp.44" will be imported as: "pcomp.44"
CQUAD4   1062    44      162     173     174     163     4       0.
CQUAD4   1063    44      161     172     173     162     4       0.
CQUAD4   1072    44      151     162     163     152     4       0.
CQUAD4   1073    44      150     161     162     151     4       0.
CQUAD4   1262    44      36      47      48      37      4       0.
CQUAD4   1263    44      37      48      49      38      4       0.
CQUAD4   1272    44      25      36      37      26      4       0.
CQUAD4   1273    44      26      37      38      27      4       0.
$ Elements and Element Properties for region : pcomp.45
$ Composite Property Record created from P3/PATRAN composite material
$ record : pcomp.50
$ Composite Material Description :
PCOMP    45      -.03            8000.   HOFF    0.      0.
         201     .015    0.      YES     202     .015    45.     YES
$ Pset: "pcomp.45" will be imported as: "pcomp.45"
CQUAD4   1082    45      140     151     152     141     4       0.
CQUAD4   1083    45      139     150     151     140     4       0.
CQUAD4   1092    45      129     140     141     130     4       0.
CQUAD4   1093    45      128     139     140     129     4       0.
CQUAD4   1282    45      14      25      26      15      4       0.
CQUAD4   1283    45      15      26      27      16      4       0.
CQUAD4   1292    45      3       14      15      4       4       0.
CQUAD4   1293    45      4       15      16      5       4       0.
$ Elements and Element Properties for region : pcomp.46
$ Composite Property Record created from P3/PATRAN composite material
$ record : pcomp.200
$ Composite Material Description :
PCOMP    46      -.0165          8000.   HOFF    0.      0.
         202     .0033   45.     YES     202     .0033   -45.    YES
         202     .0033   45.     YES     202     .0033   -45.    YES
         202     .0033   45.     YES
$ Pset: "pcomp.46" will be imported as: "pcomp.46"
CQUAD4   1000    46      230     241     111     100     4       0.
CQUAD4   1001    46      229     240     241     230     4       0.
```

CQUAD4	1004	46	226	237	238	227	4	0.
CQUAD4	1005	46	225	236	237	226	4	0.
CQUAD4	1006	46	224	235	236	225	4	0.
CQUAD4	1007	46	223	234	235	224	4	0.
CQUAD4	1008	46	222	233	234	223	4	0.
CQUAD4	1009	46	110	121	233	222	4	0.
CQUAD4	1010	46	219	230	100	89	4	0.
CQUAD4	1011	46	218	229	230	219	4	0.
CQUAD4	1014	46	215	226	227	216	4	0.
CQUAD4	1015	46	214	225	226	215	4	0.
CQUAD4	1016	46	213	224	225	214	4	0.
CQUAD4	1017	46	212	223	224	213	4	0.
CQUAD4	1018	46	211	222	223	212	4	0.
CQUAD4	1019	46	99	110	222	211	4	0.
CQUAD4	1020	46	208	219	89	78	4	0.
CQUAD4	1021	46	207	218	219	208	4	0.
CQUAD4	1024	46	204	215	216	205	4	0.
CQUAD4	1025	46	203	214	215	204	4	0.
CQUAD4	1026	46	202	213	214	203	4	0.
CQUAD4	1027	46	201	212	213	202	4	0.
CQUAD4	1028	46	200	211	212	201	4	0.
CQUAD4	1029	46	88	99	211	200	4	0.
CQUAD4	1030	46	197	208	78	67	4	0.
CQUAD4	1031	46	196	207	208	197	4	0.
CQUAD4	1034	46	193	204	205	194	4	0.
CQUAD4	1035	46	192	203	204	193	4	0.
CQUAD4	1036	46	191	202	203	192	4	0.
CQUAD4	1037	46	190	201	202	191	4	0.
CQUAD4	1038	46	189	200	201	190	4	0.
CQUAD4	1039	46	77	88	200	189	4	0.
CQUAD4	1040	46	186	197	67	56	4	0.
CQUAD4	1041	46	185	196	197	186	4	0.
CQUAD4	1044	46	182	193	194	183	4	0.
CQUAD4	1045	46	181	192	193	182	4	0.
CQUAD4	1046	46	180	191	192	181	4	0.
CQUAD4	1047	46	179	190	191	180	4	0.
CQUAD4	1048	46	178	189	190	179	4	0.
CQUAD4	1049	46	66	77	189	178	4	0.
CQUAD4	1050	46	175	186	56	45	4	0.
CQUAD4	1051	46	174	185	186	175	4	0.
CQUAD4	1054	46	171	182	183	172	4	0.
CQUAD4	1055	46	170	181	182	171	4	0.
CQUAD4	1056	46	169	180	181	170	4	0.
CQUAD4	1057	46	168	179	180	169	4	0.
CQUAD4	1058	46	167	178	179	168	4	0.
CQUAD4	1059	46	55	66	178	167	4	0.
CQUAD4	1060	46	164	175	45	34	4	0.
CQUAD4	1061	46	163	174	175	164	4	0.
CQUAD4	1064	46	160	171	172	161	4	0.
CQUAD4	1065	46	159	170	171	160	4	0.
CQUAD4	1066	46	158	169	170	159	4	0.
CQUAD4	1067	46	157	168	169	158	4	0.
CQUAD4	1070	46	153	164	34	23	4	0.
CQUAD4	1071	46	152	163	164	153	4	0.
CQUAD4	1074	46	149	160	161	150	4	0.
CQUAD4	1075	46	148	159	160	149	4	0.
CQUAD4	1076	46	147	158	159	148	4	0.

CQUAD4	1077	46	146	157	158	147	4	0.
CQUAD4	1080	46	142	153	23	12	4	0.
CQUAD4	1081	46	141	152	153	142	4	0.
CQUAD4	1084	46	138	149	150	139	4	0.
CQUAD4	1085	46	137	148	149	138	4	0.
CQUAD4	1086	46	136	147	148	137	4	0.
CQUAD4	1087	46	135	146	147	136	4	0.
CQUAD4	1088	46	134	145	146	135	4	0.
CQUAD4	1089	46	22	33	145	134	4	0.
CQUAD4	1090	46	131	142	12	1	4	0.
CQUAD4	1091	46	130	141	142	131	4	0.
CQUAD4	1094	46	127	138	139	128	4	0.
CQUAD4	1095	46	126	137	138	127	4	0.
CQUAD4	1096	46	125	136	137	126	4	0.
CQUAD4	1097	46	124	135	136	125	4	0.
CQUAD4	1098	46	123	134	135	124	4	0.
CQUAD4	1099	46	11	22	134	123	4	0.
CQUAD4	1200	46	100	111	112	101	4	0.
CQUAD4	1201	46	101	112	113	102	4	0.
CQUAD4	1204	46	104	115	116	105	4	0.
CQUAD4	1205	46	105	116	117	106	4	0.
CQUAD4	1206	46	106	117	118	107	4	0.
CQUAD4	1207	46	107	118	119	108	4	0.
CQUAD4	1208	46	108	119	120	109	4	0.
CQUAD4	1209	46	109	120	121	110	4	0.
CQUAD4	1210	46	89	100	101	90	4	0.
CQUAD4	1211	46	90	101	102	91	4	0.
CQUAD4	1214	46	93	104	105	94	4	0.
CQUAD4	1215	46	94	105	106	95	4	0.
CQUAD4	1216	46	95	106	107	96	4	0.
CQUAD4	1217	46	96	107	108	97	4	0.
CQUAD4	1218	46	97	108	109	98	4	0.
CQUAD4	1219	46	98	109	110	99	4	0.
CQUAD4	1220	46	78	89	90	79	4	0.
CQUAD4	1221	46	79	90	91	80	4	0.
CQUAD4	1224	46	82	93	94	83	4	0.
CQUAD4	1225	46	83	94	95	84	4	0.
CQUAD4	1226	46	84	95	96	85	4	0.
CQUAD4	1227	46	85	96	97	86	4	0.
CQUAD4	1228	46	86	97	98	87	4	0.
CQUAD4	1229	46	87	98	99	88	4	0.
CQUAD4	1230	46	67	78	79	68	4	0.
CQUAD4	1231	46	68	79	80	69	4	0.
CQUAD4	1234	46	71	82	83	72	4	0.
CQUAD4	1235	46	72	83	84	73	4	0.
CQUAD4	1236	46	73	84	85	74	4	0.
CQUAD4	1237	46	74	85	86	75	4	0.
CQUAD4	1238	46	75	86	87	76	4	0.
CQUAD4	1239	46	76	87	88	77	4	0.
CQUAD4	1240	46	56	67	68	57	4	0.
CQUAD4	1241	46	57	68	69	58	4	0.
CQUAD4	1244	46	60	71	72	61	4	0.
CQUAD4	1245	46	61	72	73	62	4	0.
CQUAD4	1246	46	62	73	74	63	4	0.
CQUAD4	1247	46	63	74	75	64	4	0.
CQUAD4	1248	46	64	75	76	65	4	0.
CQUAD4	1249	46	65	76	77	66	4	0.

```
CQUAD4   1250    46      45      56      57      46      4       0.
CQUAD4   1251    46      46      57      58      47      4       0.
CQUAD4   1254    46      49      60      61      50      4       0.
CQUAD4   1255    46      50      61      62      51      4       0.
CQUAD4   1256    46      51      62      63      52      4       0.
CQUAD4   1257    46      52      63      64      53      4       0.
CQUAD4   1258    46      53      64      65      54      4       0.
CQUAD4   1259    46      54      65      66      55      4       0.
CQUAD4   1260    46      34      45      46      35      4       0.
CQUAD4   1261    46      35      46      47      36      4       0.
CQUAD4   1264    46      38      49      50      39      4       0.
CQUAD4   1265    46      39      50      51      40      4       0.
CQUAD4   1266    46      40      51      52      41      4       0.
CQUAD4   1267    46      41      52      53      42      4       0.
CQUAD4   1270    46      23      34      35      24      4       0.
CQUAD4   1271    46      24      35      36      25      4       0.
CQUAD4   1274    46      27      38      39      28      4       0.
CQUAD4   1275    46      28      39      40      29      4       0.
CQUAD4   1276    46      29      40      41      30      4       0.
CQUAD4   1277    46      30      41      42      31      4       0.
CQUAD4   1280    46      12      23      24      13      4       0.
CQUAD4   1281    46      13      24      25      14      4       0.
CQUAD4   1284    46      16      27      28      17      4       0.
CQUAD4   1285    46      17      28      29      18      4       0.
CQUAD4   1286    46      18      29      30      19      4       0.
CQUAD4   1287    46      19      30      31      20      4       0.
CQUAD4   1288    46      20      31      32      21      4       0.
CQUAD4   1289    46      21      32      33      22      4       0.
CQUAD4   1290    46      1       12      13      2       4       0.
CQUAD4   1291    46      2       13      14      3       4       0.
CQUAD4   1294    46      5       16      17      6       4       0.
CQUAD4   1295    46      6       17      18      7       4       0.
CQUAD4   1296    46      7       18      19      8       4       0.
CQUAD4   1297    46      8       19      20      9       4       0.
CQUAD4   1298    46      9       20      21      10      4       0.
CQUAD4   1299    46      10      21      22      11      4       0.
$ Elements and Element Properties for region : pshell.47
PSHELL   47      601     .02     601             601
$ Pset: "pshell.47" will be imported as: "pshell.47"
CQUAD4   1068    47      302     310     311     309     4       0.
CQUAD4   1069    47      301     307     310     302     4       0.
CQUAD4   1078    47      314     302     309     308     4       0.
CQUAD4   1079    47      312     301     302     314     4       0.
CQUAD4   1268    47      304     305     306     300     4       0.
CQUAD4   1269    47      300     306     307     301     4       0.
CQUAD4   1278    47      303     304     300     313     4       0.
CQUAD4   1279    47      313     300     301     312     4       0.
$ Referenced Material Records
$ Material Record : mat1.301
$ Description of Material :
MAT1     301     13100.          .499    .0027
$ Material Record : mat1.601
$ Description of Material :
MAT1     601     2.67+6          .483333 .068
$ Material Record : mat1.701
$ Description of Material :
MAT1     701     2.+7            .3
```

```
$ Material Record : mat1.901
$ Description of Material :
MAT1     901    2.+7            .3       .058
$ Material Record : mat8.201
$ Description of Material :
MAT8     201    1.58+7  1.5+6   .28     1.+6                     .058
                                218000. 247000. 5850.   35700.  10000.
$ Material Record : mat8.202
$ Description of Material :
MAT8     202    2.67+6  2.67+6          500000.                  .068
                                43000.  45000.  43000.  45000.  10000.
$ Material Record : mat8.501
$ Description of Material :
MAT8     501    2.67+6  2.67+6  .3      500000.                  .068
$ Multipoint Constraints of Group : left_wing
RBE2     303     304     123     42
RBE2     304     303     123     31
RBE2     421     403     123456  112     113     114     115     116
         117     118     119     234     235     236     237     238
         239     240     241
RBE2     4429    518     123456  9       10      123     124
RBE2     4430    511     123456  2       131
RBE2     4431    512     123456  3       130
RBE2     4432    513     123456  4       129
RBE2     4433    514     123456  5       128
RBE2     4434    305     123     53
RBE2     5000    307     123456  55
RBE2     5001    312     123456  33
RBE2     5002    167     123456  310
RBE2     5003    54      123456  306
RBE2     5004    145     123456  314
RBE2     5005    32      123456  313
RBE2     5006    146     123456  308
RBE2     5007    168     123456  311
$ Nodes of Group : left_wing
GRID     1              19.125  -18.    1.57-6
GRID     2              19.9853 -18.    -.104989 3
GRID     3              20.8561 -18.    -.142824 3
GRID     4              21.7274 -18.    -.164471 3
GRID     5              22.5989 -18.    -.173716 3
GRID     6              23.4706 -18.    -.170052
GRID     7              24.3419 -18.    -.151726
GRID     8              25.2129 -18.    -.122049
GRID     9              26.084  -18.    -.084171 5
GRID     10             26.9545 -18.    -.042647 3
GRID     11             27.825  -18.    -7.81-4
GRID     12             17.2125 -16.2   1.41-6
GRID     13             18.1175 -16.2   -.110423
GRID     14             19.0331 -16.2   -.150214
GRID     15             19.9494 -16.2   -.172979
GRID     16             20.8661 -16.2   -.182702
GRID     17             21.7829 -16.2   -.178847
GRID     18             22.6993 -16.2   -.159573
GRID     19             23.6154 -16.2   -.128362
GRID     20             24.5315 -16.2   -.088525
GRID     21             25.447  -16.2   -.044854
GRID     22             26.3624 -16.2   -8.22-4
```

```
GRID    23              15.3    -14.4   1.25-6
GRID    24              16.2495 -14.4   -.115857
GRID    25              17.2103 -14.4   -.157603
GRID    26              18.1717 -14.4   -.181487
GRID    27              19.1334 -14.4   -.191687
GRID    28              20.0952 -14.4   -.187643
GRID    29              21.0566 -14.4   -.167421
GRID    30              22.0177 -14.4   -.134674
GRID    31              22.9789 -14.4   -.09288 3
GRID    32              23.9395 -14.4   -.047061
GRID    33              24.9    -14.4   -8.62-4
GRID    34              13.3875 -12.59991.1-6
GRID    35              14.3816 -12.5999-.121291
GRID    36              15.3874 -12.5999-.164993
GRID    37              16.3939 -12.5999-.189996
GRID    38              17.4006 -12.5999-.200673
GRID    39              18.4074 -12.5999-.196439
GRID    40              19.414  -12.5999-.175268
GRID    41              20.4203 -12.5999-.140986
GRID    42              21.4263 -12.5999-.097234 3
GRID    45              11.475  -10.8   9.44-7
GRID    46              12.5137 -10.8   -.126726
GRID    47              13.5645 -10.8   -.172384
GRID    48              14.616  -10.8   -.198504
GRID    49              15.6679 -10.8   -.209659
GRID    50              16.7199 -10.8   -.205234
GRID    51              17.7714 -10.8   -.183115
GRID    52              18.8227 -10.8   -.147297
GRID    53              19.8738 -10.7999-.101589 3
GRID    54              20.9244 -10.7999-.051475
GRID    55              21.975  -10.7999-9.44-4
GRID    56              9.5625  -9.     7.86-7
GRID    57              10.6458 -9.     -.132161
GRID    58              11.7416 -9.     -.179774
GRID    59              12.8382 -9.     -.207013
GRID    60              13.9351 -9.     -.218645
GRID    61              15.0322 -9.     -.21403
GRID    62              16.1287 -9.     -.190961
GRID    63              17.2251 -9.     -.153609
GRID    64              18.3211 -9.     -.105944
GRID    65              19.4169 -9.     -.053681
GRID    66              20.5125 -9.     -9.84-4
GRID    67              7.65    -7.2    6.29-7
GRID    68              8.77792 -7.2    -.137596
GRID    69              9.91882 -7.2    -.187164
GRID    70              11.0604 -7.2    -.215522
GRID    71              12.2024 -7.2    -.227631
GRID    72              13.3445 -7.2    -.222825
GRID    73              14.4862 -7.2    -.198808
GRID    74              15.6276 -7.2    -.159921
GRID    75              16.7687 -7.2    -.110298
GRID    76              17.9093 -7.2    -.055889
GRID    77              19.0499 -7.2    -.001025
GRID    78              5.7375  -5.4    4.72-7
GRID    79              6.91001 -5.4    -.143032
GRID    80              8.09596 -5.4    -.194555
GRID    81              9.28267 -5.4    -.224031
```

```
GRID    82              10.4697 -5.4    -.236616
GRID    83              11.6568 -5.4    -.231621
GRID    84              12.8436 -5.4    -.206655
GRID    85              14.03   -5.4    -.166233
GRID    86              15.2161 -5.4    -.114653
GRID    87              16.4018 -5.4    -.058096
GRID    88              17.5875 -5.4    -.001066
GRID    89              3.825   -3.6    3.14-7
GRID    90              5.04211 -3.6    -.148468
GRID    91              6.27309 -3.6    -.201946
GRID    92              7.50487 -3.6    -.23254
GRID    93              8.73697 -3.6    -.245602
GRID    94              9.96917 -3.59999-.240416
GRID    95              11.201  -3.59999-.214501
GRID    96              12.4324 -3.59999-.172544
GRID    97              13.6635 -3.59999-.119008
GRID    98              14.8943 -3.59999-.060303
GRID    99              16.125  -3.59999-.001107
GRID    100             1.91249 -1.799991.57-7
GRID    101             3.17421 -1.79999-.153904
GRID    102             4.45024 -1.79999-.209337
GRID    103             5.72708 -1.79999-.241049
GRID    104             7.00424 -1.79999-.254588
GRID    105             8.28149 -1.8    -.249212
GRID    106             9.55843 -1.8    -.222348
GRID    107             10.8349 -1.8    -.178856
GRID    108             12.1109 -1.8    -.123363
GRID    109             13.3867 -1.8    -.06251
GRID    110             14.6625 -1.8    -.001147
GRID    111              0.      0.      0.
GRID    112             1.30632 -1.39-8 -.159341 3
GRID    113             2.62739 -1.89-8 -.216728 3
GRID    114             3.94929 -2.18-8 -.249558 3
GRID    115             5.27152 -2.3-8  -.263574 3
GRID    116             6.59382 -2.25-8 -.258007 3
GRID    117             7.91583 -2.01-8 -.230194 3
GRID    118             9.23737 -1.61-8 -.185167 3
GRID    119             10.5584 -1.11-8 -.127718 3
GRID    120             11.8792 -5.65-9 -.064717
GRID    121             13.2    -1.03-10-.001188
GRID    123             26.9543 -18.    .042659  3
GRID    124             26.0837 -18.    .084186  3
GRID    125             25.2129 -18.    .122052
GRID    126             24.3419 -18.    .151729
GRID    127             23.4705 -18.    .170056
GRID    128             22.5989 -18.    .173719  3
GRID    129             21.7274 -18.    .164474  3
GRID    130             20.8561 -18.    .142827  3
GRID    131             19.9853 -18.    .104987  3
GRID    134             25.4468 -16.1999.044865
GRID    135             24.5312 -16.1999.08854
GRID    136             23.6154 -16.1999.128364
GRID    137             22.6993 -16.1999.159576
GRID    138             21.7828 -16.1999.178852
GRID    139             20.8661 -16.1999.182705
GRID    140             19.9494 -16.1999.172982
GRID    141             19.0331 -16.1999.150216
```

```
GRID     142            18.1173 -16.1999.11042
GRID     145            23.9393 -14.3999.047071
GRID     146            22.9786 -14.3999.092893
GRID     147            22.0177 -14.3999.134676
GRID     148            21.0566 -14.3999.167423
GRID     149            20.0951 -14.3999.187647
GRID     150            19.1334 -14.3999.19169
GRID     151            18.1717 -14.3999.18149
GRID     152            17.2103 -14.3999.157606
GRID     153            16.2493 -14.3999.115854
GRID     157            21.4261 -12.5999.097247
GRID     158            20.4202 -12.5999.140987
GRID     159            19.414  -12.5999.17527
GRID     160            18.4074 -12.5999.196442
GRID     161            17.4006 -12.5999.200676
GRID     162            16.3939 -12.5999.189999
GRID     163            15.3874 -12.5999.164995
GRID     164            14.3815 -12.5999.121288
GRID     167            20.9242 -10.7999.051483
GRID     168            19.8735 -10.7999.1016
GRID     169            18.8227 -10.7999.147299
GRID     170            17.7714 -10.7999.183116
GRID     171            16.7197 -10.7999.205237
GRID     172            15.6679 -10.7999.209661
GRID     173            14.616  -10.7999.198507
GRID     174            13.5645 -10.7999.172385
GRID     175            12.5136 -10.7999.126723
GRID     178            19.4167 -8.99993.053689
GRID     179            18.3209 -8.99993.105953
GRID     180            17.2251 -8.99994.153611
GRID     181            16.1287 -8.99995.190963
GRID     182            15.032  -8.99996.214033
GRID     183            13.9351 -8.99996.218647
GRID     184            12.8382 -8.99997.207015
GRID     185            11.7416 -8.99998.179775
GRID     186            10.6457 -8.99999.132158
GRID     189            17.9092 -7.19992.055895
GRID     190            16.7684 -7.19993.110306
GRID     191            15.6275 -7.19994.159922
GRID     192            14.4861 -7.19995.19881
GRID     193            13.3444 -7.19996.222828
GRID     194            12.2024 -7.19996.227632
GRID     195            11.0604 -7.19997.215523
GRID     196            9.91878 -7.19998.187165
GRID     197            8.77783 -7.19999.137593
GRID     200            16.4016 -5.39992.0581
GRID     201            15.2159 -5.39993.11466
GRID     202            14.0299 -5.39994.166234
GRID     203            12.8435 -5.39995.206656
GRID     204            11.6567 -5.39995.231623
GRID     205            10.4696 -5.39996.236618
GRID     206            9.28263 -5.39997.224032
GRID     207            8.0959  -5.39998.194555
GRID     208            6.90992 -5.39999.143028
GRID     211            14.8941 -3.59992.060306
GRID     212            13.6634 -3.59993.119013
GRID     213            12.4324 -3.59993.172545
```

```
GRID    214             11.2009 -3.59994.214503
GRID    215             9.96907 -3.59995.240418
GRID    216             8.73691 -3.59996.245603
GRID    217             7.50482 -3.59997.23254
GRID    218             6.27304 -3.59998.201945
GRID    219             5.04203 -3.59999.148464
GRID    222             13.3866 -1.79991.062512
GRID    223             12.1108 -1.79992.123366
GRID    224             10.8348 -1.79993.178857
GRID    225             9.55836 -1.79994.222349
GRID    226             8.2814  -1.79995.249213
GRID    227             7.00418 -1.79996.254589
GRID    228             5.72702 -1.79997.241049
GRID    229             4.45017 -1.79998.209336
GRID    230             3.17414 -1.79999.153901
GRID    233             11.8792 5.65-9  .064717
GRID    234             10.5584 1.11-8  .127719  3
GRID    235             9.23735 1.61-8  .185168  3
GRID    236             7.9158  2.01-8  .230195  3
GRID    237             6.59378 2.25-8  .258007  3
GRID    238             5.27148 2.3-8   .263574  3
GRID    239             3.94924 2.18-8  .249557  3
GRID    240             2.62734 1.89-8  .216727  3
GRID    241             1.30626 1.39-8  .159337  3
GRID    300             22.4319 -12.5999-.049268
GRID    301             23.4375 -12.5999-9.03-4
GRID    302             22.4317 -12.5999.049277
GRID    303             22.9789 -14.4   -.09288  5
GRID    304             21.4263 -12.5999-.097234 5
GRID    305             19.8738 -10.7999-.101589 5
GRID    306             20.9244 -10.7999-.051475
GRID    307             21.975  -10.7999-9.44-4
GRID    308             22.9786 -14.3999.092893
GRID    309             21.4261 -12.5999.097247
GRID    310             20.9242 -10.7999.051483
GRID    311             19.8735 -10.7999.1016
GRID    312             24.9    -14.4   -8.62-4
GRID    313             23.9395 -14.4   -.047061
GRID    314             23.9393 -14.3999.047071
GRID    402             3.94929  0.      0.      3
GRID    403             3.94929  0.      0.      3
GRID    500             12.75   -18.5    0.
GRID    501             14.50   -18.5   1.57-7
GRID    502             15.125  -18.5   3.14-7
GRID    503             15.625  -18.5   4.71-7
GRID    504             16.125  -18.5   6.28-7
GRID    505             16.50   -18.5   7.85-7
GRID    506             17.125  -18.5   9.42-7
GRID    507             17.625  -18.5   1.09-6
GRID    508             18.125  -18.5   1.25-6
GRID    509             18.625  -18.5   1.41-6
GRID    510             19.125  -18.5   1.57-6
GRID    511             20.0569 -18.5   1.46-6   3
GRID    512             20.9888 -18.5   1.35-6   3
GRID    513             21.9207 -18.5   1.24-6   3
GRID    514             22.8526 -18.5   1.14-6   3
GRID    515             23.7845 -18.5   1.03-6
```

```
GRID     516            24.7164 -18.5   9.29-7
GRID     517            25.6483 -18.5   8.22-7
GRID     518            26.7366 -18.5   6.97-7   3
GRID     519            27.825  -18.5   5.72-7
GRID     520            28.325  -18.5   5.15-7
GRID     521            28.825  -18.5   4.58-7
GRID     522            29.325  -18.5   4.01-7
GRID     523            29.825  -18.5   3.43-7
GRID     524            30.325  -18.5   2.86-7
GRID     525            30.825  -18.5   2.29-7
GRID     526            31.325  -18.5   1.71-7
GRID     527            31.825  -18.5   1.14-7
GRID     528            32.325  -18.5   5.72-8
GRID     529            32.825  -18.5    0.
GRID     530            19.5909 -18.5   1.51-6
$ Loads for Load Case :
SPCADD   2       100
$ Displacement Constraints of Load Set : spc1.100
SPC1     100     123456  402
$ Referenced Coordinate Frames
CORD2R   3               0.      0.      0.      0.      0.     1.
        -1.      0.      0.
CORD2R   4               0.      0.      0.     -.707107-.707107-3.079-8
        -.707107.707107 3.079-8
CORD2R   5              19.8738 -10.7999-.10158934.647  -27.9279-.060154
        2.77994 -25.547 -1.49394
$
$ASET1    3       12      22      23      34      45      56
$ASET1    3       66      67      77      78      88      89
$ASET1    3       99      100     110     111     121     500
$ASET1    3       510     529
ENDDATA b46081d2
```

REPORT DOCUMENTATION PAGE

Form Approved OMB No. 0704-0188

1. REPORT DATE *(DD-MM-YYYY)*	2. REPORT TYPE	3. DATES COVERED *(From - To)*
01-04-2009	Technical Memorandum	

4. TITLE AND SUBTITLE
Updating the Finite Element Model of the Aerostructures Test Wing Using Ground Vibration Test Data

5a. CONTRACT NUMBER

5b. GRANT NUMBER

5c. PROGRAM ELEMENT NUMBER

6. AUTHOR(S)
Lung, Shun-Fat and Pak, Chan-Gi

5d. PROJECT NUMBER

5e. TASK NUMBER

5f. WORK UNIT NUMBER

7. PERFORMING ORGANIZATION NAME(S) AND ADDRESS(ES)
NASA Dryden Flight Research Center
P.O. Box 273
Edwards, California 93523-0273

8. PERFORMING ORGANIZATION REPORT NUMBER
H-2942

9. SPONSORING/MONITORING AGENCY NAME(S) AND ADDRESS(ES)
National Aeronautics and Space Administration
Washington, DC 20546-0001

10. SPONSORING/MONITOR'S ACRONYM(S)
NASA

11. SPONSORING/MONITORING REPORT NUMBER
NASA/TM-2009-214646

12. DISTRIBUTION/AVAILABILITY STATEMENT
Unclassifed -- Unlimited
Subject Category 01 Availability: NASA CASI (301) 621-0390 Distribution: Standard

13. SUPPLEMENTARY NOTES
Lung, TYBRIN, Inc.; Pak, NASA Dryden Flight Research Center. An Electronic version can be found at http://dtrs.dfrc.nasa.gov or http://ntrs.nasa.gov/search.jsp

14. ABSTRACT
Improved and/or accelerated decision making is a crucial step during flutter certification processes. Unfortunately, most finite element structural dynamics models have uncertainties associated with model validity. Tuning the finite element model using measured data to minimize the model uncertainties is a challenging task in the area of structural dynamics. The model tuning process requires not only satisfactory correlations between analytical and experimental results, but also the retention of the mass and stiffness properties of the structures. Minimizing the difference between analytical and experimental results is a type of optimization problem. By utilizing the multidisciplinary design, analysis, and optimization (MDAO) tool in order to optimize the objective function and constraints; the mass properties, the natural frequencies, and the mode shapes can be matched to the target data to retain the mass matrix orthogonality. This approach has been applied to minimize the model uncertainties for the structural dynamics model of the aerostructures test wing (ATW), which was designed and tested at the National Aeronautics and Space Administration Dryden Flight Research Center (Edwards, California). This study has shown that natural frequencies and corresponding mode shapes from the updated finite element model have excellent agreement with corresponding measured data.

15. SUBJECT TERMS
Aerostructures test wing, Ground vibration test, Multidisciplinary design, analysis, and optimization, Structural dynamic model tuning, Sensor/Actuator placement

16. SECURITY CLASSIFICATION OF: a. REPORT	b. ABSTRACT	c. THIS PAGE	17. LIMITATION OF ABSTRACT	18. NUMBER OF PAGES	19b. NAME OF RESPONSIBLE PERSON / 19b. TELEPHONE NUMBER *(Include area code)*
U	U	U	UU	43	STI Help Desk (email:help@sti.nasa.gov) / (301) 621-0390